

See discussions, stats, and author profiles for this publication at: <https://www.researchgate.net/publication/277392423>

# Seismic Inversion Methods and some of their constraints

Article in *First Break* · June 2004

DOI: 10.3997/1365-2397.2004011

---

CITATIONS

52

---

READS

293

2 authors, including:



Paul C. H. Veeken

Wintershall

57 PUBLICATIONS 295 CITATIONS

SEE PROFILE

Some of the authors of this publication are also working on these related projects:



Borehole CSEM [View project](#)



seismic stratigraphic textbook [View project](#)

All content following this page was uploaded by [Paul C. H. Veeken](#) on 16 October 2017.

The user has requested enhancement of the downloaded file.

# Seismic inversion methods and some of their constraints

P. C. H. Veeken and M. Da Silva\*

## Introduction

The interest in seismic inversion techniques has been growing steadily over the last couple of years. Integrated studies are essential to hydrocarbon development projects (e.g. Vazquez *et al.* 1997, Cosentino 2001) and inversion is one of the means to extract additional information from seismic data. Various seismic inversion techniques are briefly presented. Inversion replaces the seismic signature by a blocky response, corresponding to acoustic and/or elastic impedance layering. It facilitates the interpretation of meaningful geological and petrophysical boundaries in the subsurface. Inversion increases the resolution of conventional seismics in many cases and puts the study of reservoir parameters at a different level. It results in optimised volumetrics, improved ranking of leads/prospects, better delineation of drainage areas and identification of 'sweet spots' in field development studies (e.g. Veeken *et al.* 2002).

The main steps in an inversion study are:

- Quality control and pre-conditioning of the input data.
- Well-to-seismic match, zero-phasing of data in zone of interest and extraction of the wavelet.
- Running of the inversion algorithm with generation of acoustic or elastic impedance cubes and extraction of attributes.
- Visualisation and interpretation of the results in terms of reservoir development.

The inversion methods are either deterministic or probabilistic and the approach can be post- and/or pre-stack. Inversion schemes generally use migrated time data as basic input. The pre-stack method exploits AVO effects on migrated CDP gathers. There is a trade-off between method/cost/time and quality of inversion results. Feasibility studies with synthetic modelling are recommended before embarking on an inversion or AVO project (Da Silva *et al.*, in prep.).

The past track record has demonstrated the benefits of the seismic inversion method. However, it should be realised that the inversion procedure is not a unique process, i.e. there is no one single solution to the given problem. Care should be taken when interpreting the inversion results. Adequate data pre-conditioning is a prerequisite for quantitative interpretation of the end results.

## Deconvolution and seismic inversion.

Seismic inversion is undertaken to complement conventional deconvolution processing. Deconvolution tries to undo some

negative effects of the seismic convolution. It is in general successful in reducing multiple energy (Yilmaz 2001). During acquisition of reflection datasets, the seismic signal is sent through the earth (i.e. convolved with the earth filter) and reflected back into the geophone (convolved with the recording set-up filter). Deconvolution is meant to undo the deformation caused by these two filters to the seismic response. A spiked response is never achieved because of the band limited nature of the seismic data (Veeken, in prep.). The decon filter would need to be infinitely long, which is clearly not feasible. A perfect job is therefore hardly ever possible and that is where seismic inversion or stratigraphic deconvolution comes in.

Ideally, an acoustic impedance interface should be represented by a single spike on the seismic trace. The contrast is described by the reflectivity formula:

$$R = (\rho_2 V_2 - \rho_1 V_1) / (\rho_2 V_2 + \rho_1 V_1) \quad (1)$$

Acoustic impedance interfaces in the real world are sometimes positioned very closely together. As a result, the seismic response of the first interface overlaps in time with the energy triggered by the next interface. The result is interference of the individual seismic events on the recorded seismogram. A composite seismic loop is registered in the geophone at the surface (Figure 1A). Under these circumstances it becomes difficult to discriminate between the effects stemming from each interface. Therefore, the apparent amplitude and frequency of reflections should always be treated with care during the interpretation phase (Veeken, in prep.).

It is necessary to undertake 'stratigraphic deconvolution' to undo some of the negative interference effects (cf Duboz *et al.* 1998). This technique is also known as seismic inversion. The seismic signature is replaced by a blocky response corresponding to the seismic impedance layering. This type of processing facilitates the interpretation of meaningful geological and petrophysical boundaries on the reflection data (Veeken *et al.* 2002). The input for seismic inversion is traditionally composed of time migrated seismic data (pre- or post-stack), a wavelet and an optional initial earth model (velocities and densities; Figure 1B). Inversion allows the study of reservoir characteristics in greater detail, under favourable circumstances the resolution of the dataset is even increased. Detection of thin beds is based on subtle changes in the shape of a specific seismic loop (doublet), a feature that is usually beyond the standard seismic resolution.

It is recommendable that prestack time migration data

\* P.C.H. Veeken, 29 rue des Benedictins, 57050 Le Ban St. Martin, France

M. da Silva, 1 rue Léon Migaux, 91341 Massy CEDEX, France

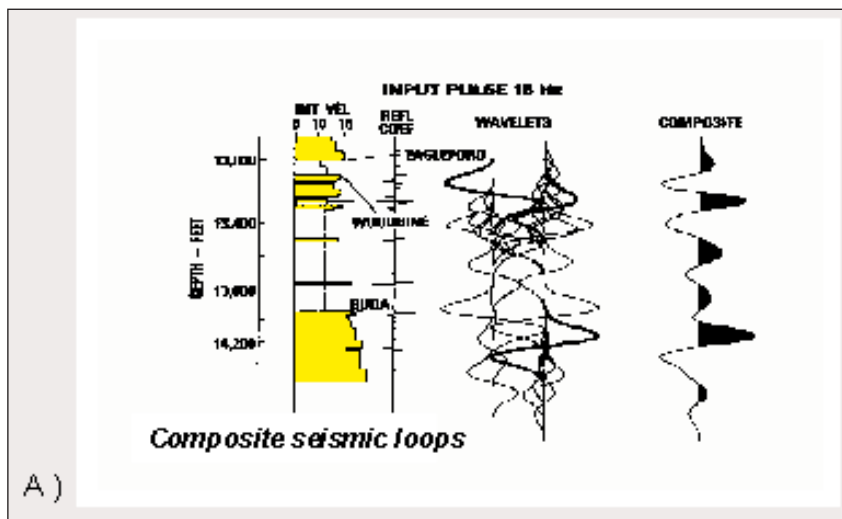


Figure 1A Thin bed configuration gives rise to a composite seismic response due to time overlap and interference of the reflected seismic pulses (modified after Todd and Sangree, 1977).

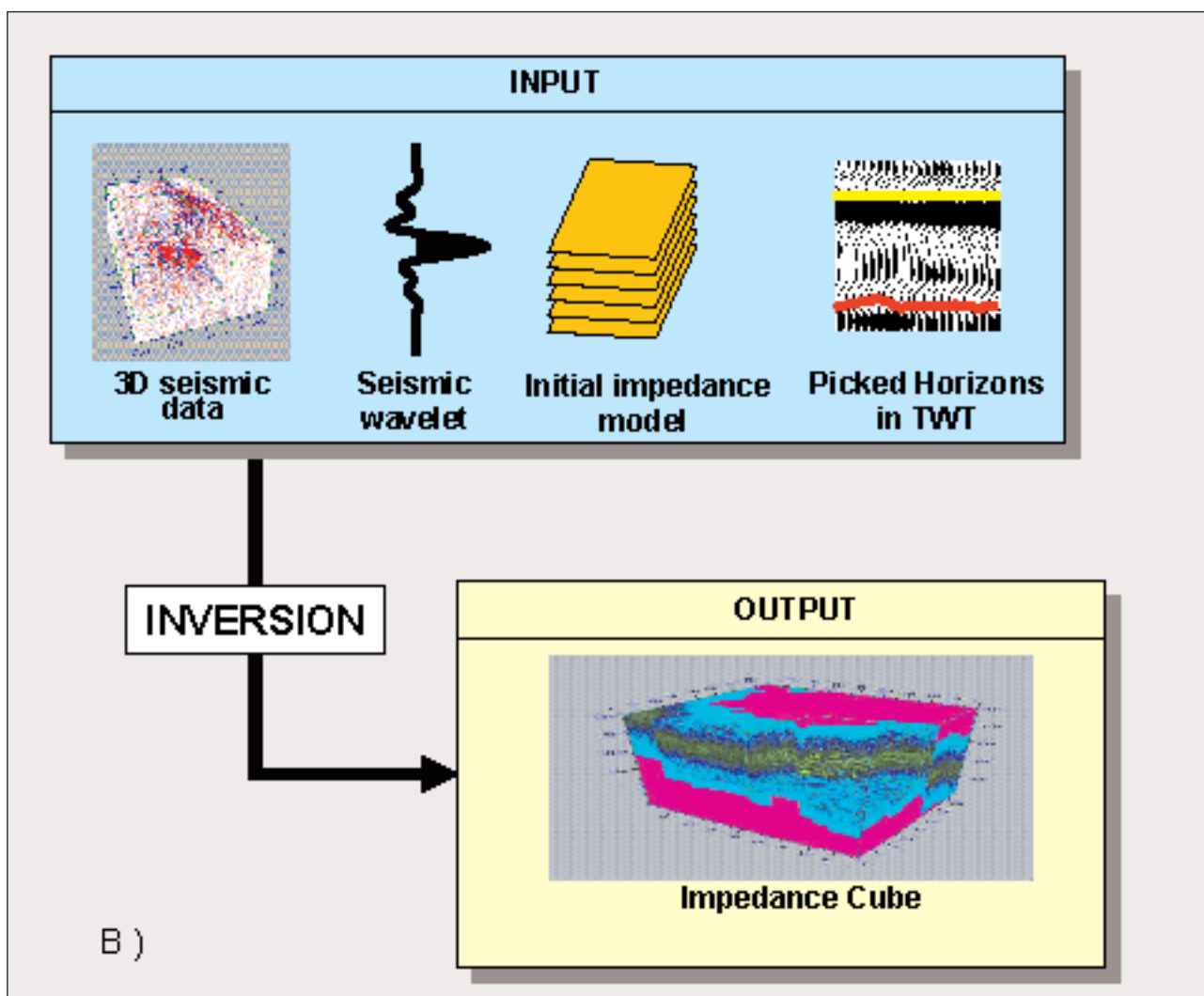
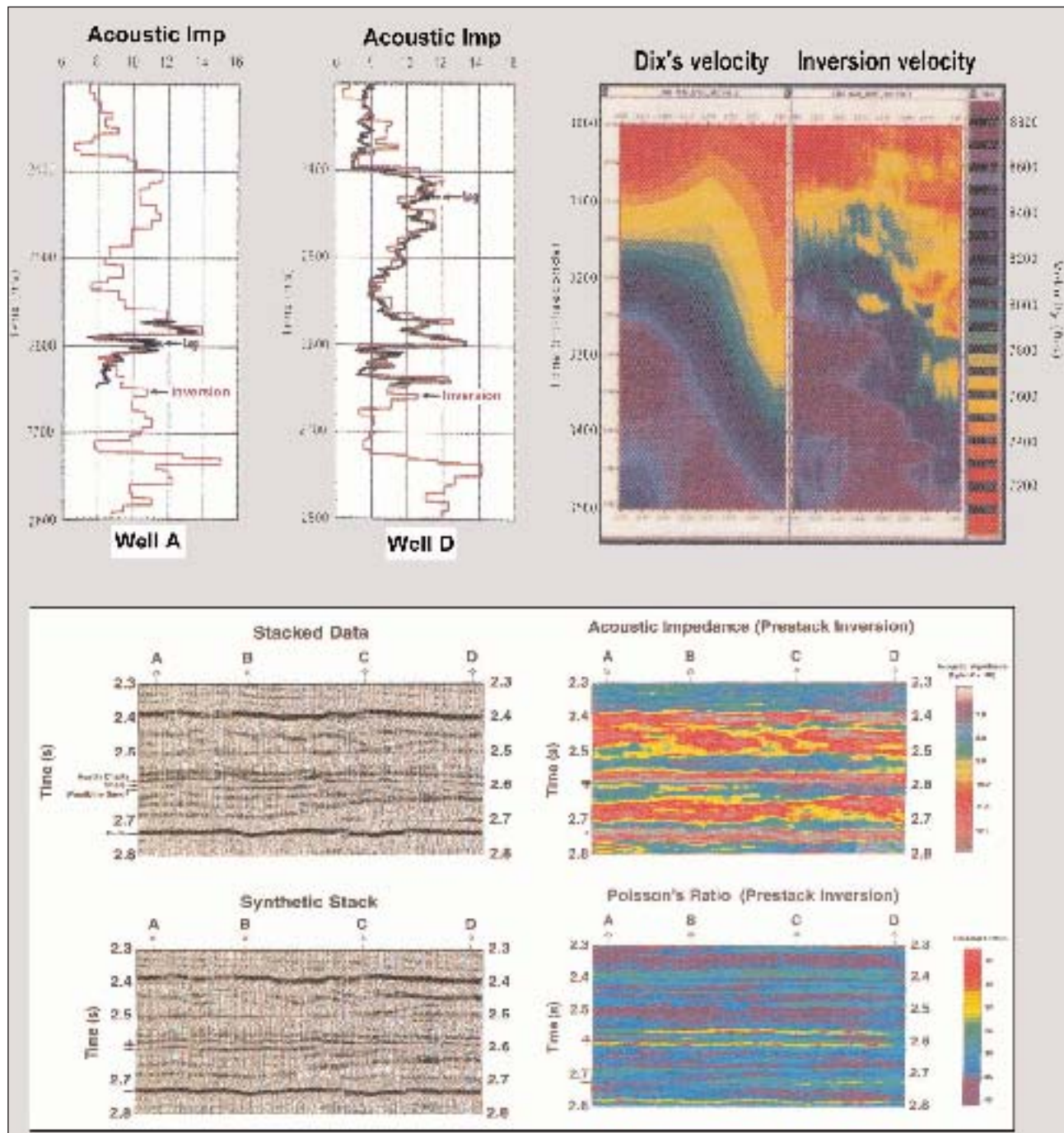


Figure 1B The input for a model-driven seismic inversion consists of time migrated seismic data, a seismic wavelet, an optional impedance model and picked time horizons. Proper data conditioning is a pre-requisite to obtain reliable results. Seismic inversion is never a unique process, i.e. there is not a single solution to the given problem, but several models may equally well explain the recorded seismic response.

serves as input to the inversion scheme. The main advantage is a substantially better velocity field and improved positioning of the reflections. The corresponding interval velocity model is in general more detailed than that obtained via the conventional seismic method exploiting Dix's formula (Dix 1955). Moreover, this velocity field is better suited for evaluation of in-situ geo-pressures and fault compartment predictions (e.g.

Dutta 2002; Figure 2).

Inversion is often done in conjunction with AVO analysis. The combination of these geophysical study techniques augments the confidence in correct ranking of leads / prospects and definition of 'sweet spots' in the HC accumulations (Veeken *et al.* 2002). Such an approach reduces uncertainties and drilling risks, which is an important aspect for optimising



**Figure 2** The pre-stack seismic inversion results in a better velocity model. The interval velocities calculated via Dix's formula are very smooth and therefore less reliable. It ensures the best stack, but does not yield necessarily the best interval velocity. The inversion involves a pre-stack time migration and this velocity model preserves better the original variability of the velocity field (modified after Dutta 2002).



an exploration and hydrocarbon development strategy (Da Silva *et al.*, in prep). A pre-stack inversion scheme incorporates AVO effects seen on CDP gathers. The partial stacks (PS) show in many cases a characteristic difference in behaviour for the amplitude of the top hydrocarbon reservoir reflection (AVO effect). The P- and S-wave energy are crucial parameters to model the reflectivity of synthetic offset gathers. Compressional P-waves contain information on the lithology and the porefill, while transverse S-waves are hardly influenced by the fluid contents. Absence of P-wave related DHIs on the corresponding S-sections is, for instance, a useful criterion to discriminate between a hydrocarbon and brine filled reservoir (Stewart *et al.* 2003). Rock physical parameters like the Poisson's ratio,  $\rho$ ,  $\lambda$ ,  $\mu$  are estimated from the P- and S-wave velocity variations. The prestack inversion gives a better handle on the lithology, porosity, permeability and/or water saturation in the porefill of the rocks under investigation.

Stratigraphic deconvolution tries to put a simple spiked reflectivity response at geological boundaries (lithological changes) and the main reservoir interfaces (for instance, a fluid contact). This is often done by inversion of the seismic cube into an acoustic impedance cube (Figure 1B). The acoustic

impedance of a rock sequence is defined as the product of density and velocity (cf Sheriff 2002). The link between the seismic and acoustic impedance (AI) cube is the seismic wavelet. The wavelet is derived either directly from the seismic data or computed with the aid of available well data. The density and sonic logs in the well permit calculation of the AI response. Calibrated sonic with checkshots and/or VSP data are needed for the depth-time conversion of the vertical log scale. The real seismic trace at the well location is subsequently matched with the reflectivity trace computed from the well logs. This comparison yields the seismic wavelet.

A typical inversion project generally comprises the following steps:

- Quality control and pre-conditioning of the input data.
- Well-to-seismic match and compilation of a synthetic trace.
- Zero-phasing of data in zone of interest and extraction of the wavelet. This step can be circumvented when the non zero-phase effects are integrated in the wavelet used for the inversion.
- Running of the inversion algorithm.
- Visualisation and interpretation of the results in terms of reservoir development.

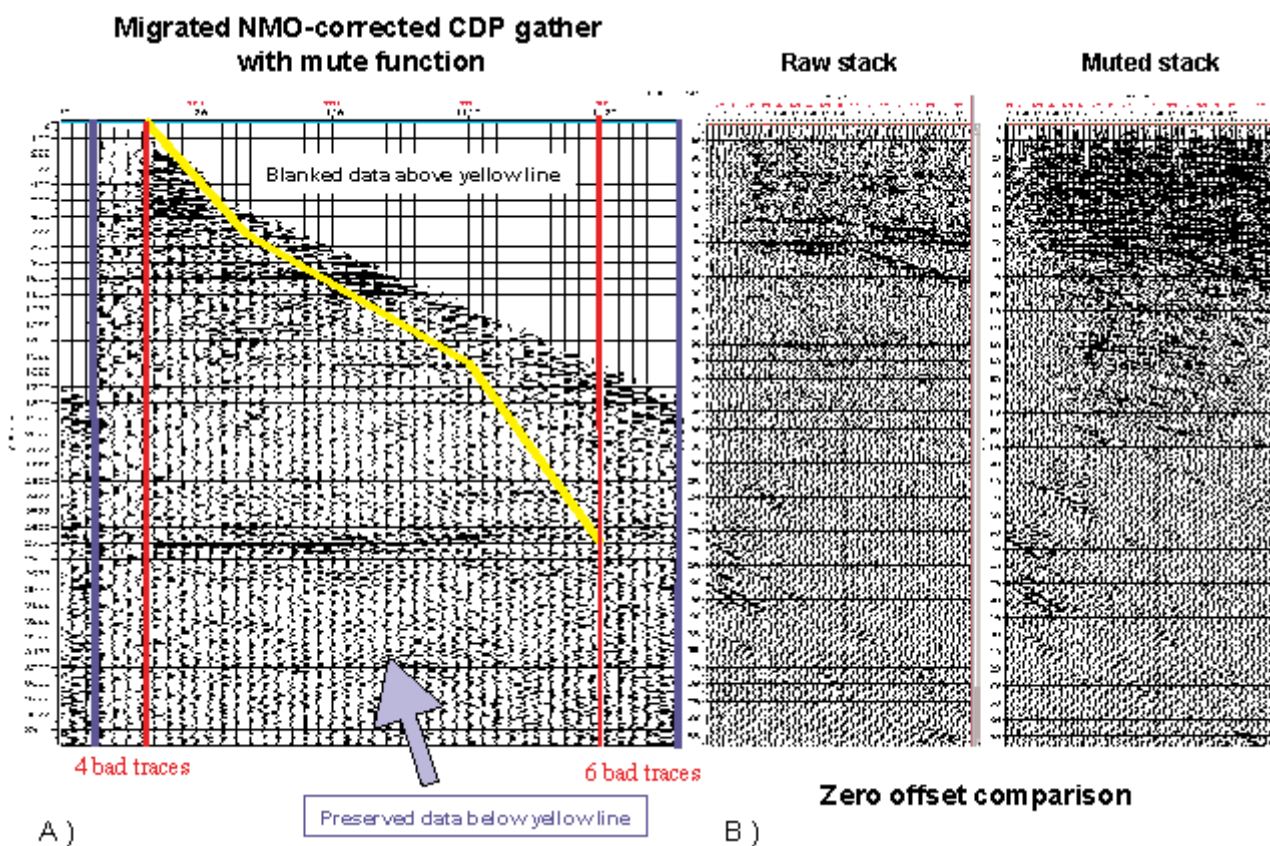
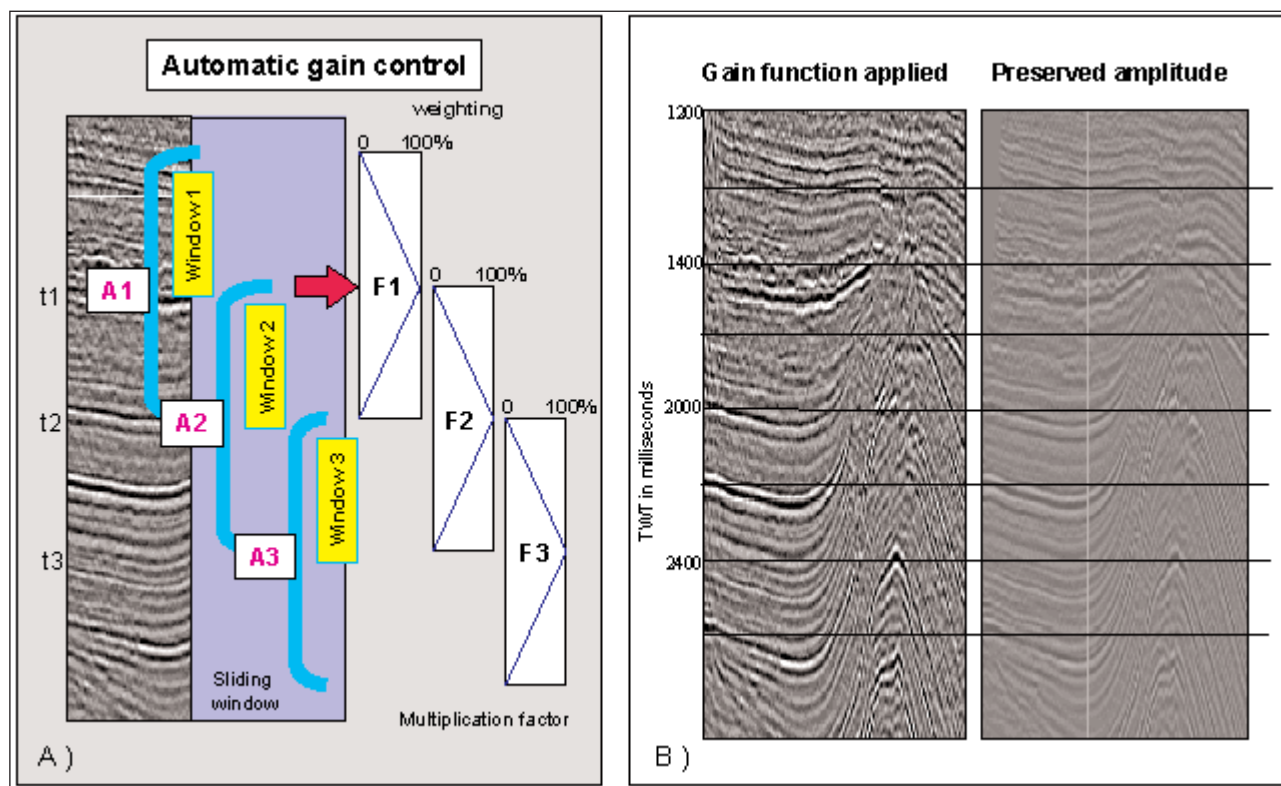


Figure 3A Mute function applied on a CDP gather. Data from a specific offset and time range is used for each time sample in the processing. In this way the amount of noise on the traces is drastically reduced. Selection of the proper mute function is critical in optimising the stacking results.

Figure 3B Comparison of a raw stacked seismic line and the same line whereby the mute function is applied on the CDP gathers before the stack.



**Figure 4A** Automatic Gain Control function (AGC) is computed in a sliding window. The average amplitude within the window (A1) is determined and scaled to a specific value. This scaling factor (F1) is applied on the sample at the centre of the window. Subsequent tapering of the multiplication factors in the overlap areas of consecutive time window positions ensures a smooth curve for the gain factors on the whole trace for each time sample. The original amplitudes are thus altered in a time variant manner.

**Figure 4B** 'Preserved amplitude' stack section compared with a normalised stack section. The preserved amplitude processing gives a better representation of the gross lithology of individual seismic units and facilitates their correct interpretation (data courtesy Pemex).

Seismic inversion is a somewhat confusing expression. Inversion in itself means to *undo an operation*, but here it represents the transformation of a seismic amplitude cube into an acoustic (or elastic) impedance cube. There are several ways to achieve this objective, as will be shown later on.

Time lapse inversion of 4D seismics and reservoir behaviour monitoring facilitate the extraction of saturation and pressure effects induced by hydrocarbon production (e.g. Gluck 2000, Oldenziel 2003).

### Input data conditioning

It is important that the seismic input data are screened for their quality. In a pre-stack approach it means going back to the CDP gathers and making sure that the panels are clean. It might prove necessary to apply a more efficient mute function for this purpose (Figure 3). Simple bandpass filtering can be very effective for improving the seismic data. Applying a spiking random noise attenuator is a more sophisticated way to reduce the noise on the migrated stack. A 3D filtering approach will give even better results (Da Silva *et al.*, in prep).

The acquisition footprint is often difficult to remove in 3D surveys, but it is an essential step for reconstituting the true amplitude character of a dataset. The aim is to preserve the real amplitude behaviour proportional to the acoustic impedance contrasts in the subsurface and eliminate any known amplitude distortions. These amplitude corrections should be implemented when it enhances the overall quality of the seismic dataset. Whitening of the amplitude spectra is in this respect sometimes a dangerous operation that needs careful evaluation before it is done. Whitening means that the amplitudes for all frequencies are adjusted to the same output level. This artificial amplitude boosting is in many cases rather uncontrolled and accompanied by a significant and unacceptable increase in noise level.

A gain function is certainly useful, unless it destroys the preserved amplitude character of the dataset (Figure 4). Preserved amplitude processing implies that only a light gain function is utilised, applied in a fairly large time window. The sliding window should preferably not be smaller than 1000 ms. Each time the sample on the seismic trace has a certain multiplication factor assigned. Amplitude balancing is a

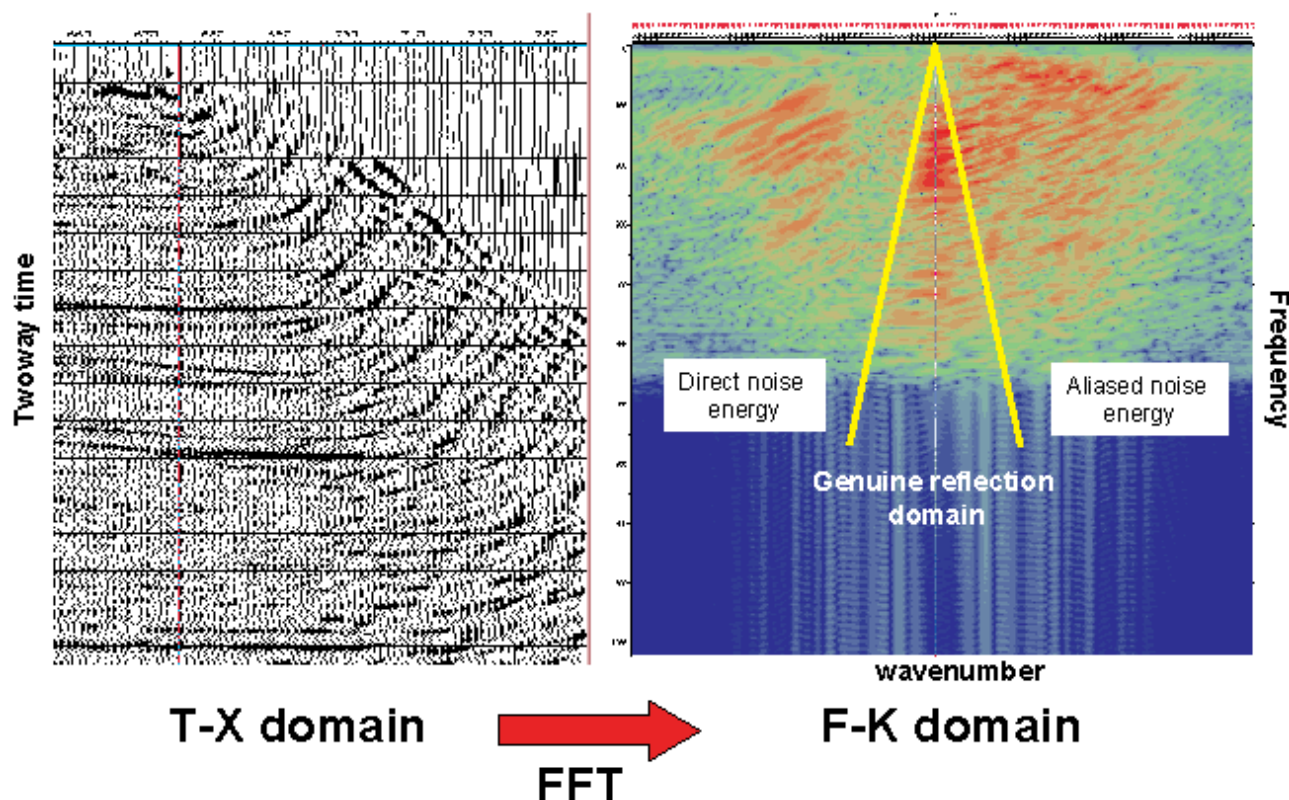


Figure 5 F-K filtering can be safely applied when it is sure that only the noise is affected by the operation. It will change the amplitude value and take out the noise distortion. It restores the amplitudes to a more reliable value that leaves scope for quantitative interpretation.

delicate process that should be done with care, especially when later quantitative interpretation is the ultimate goal (Veeken, in prep.).

Even velocity filtering is worthwhile considering on the condition that the F-K operation cuts out only noise (Figure 5). Under such circumstances the F-K filter will indeed alter the amplitudes, but in a good sense. The latter has to be demonstrated by proper testing of the processing parameters. Multiple suppression and deconvolution are other issues that need to be addressed in order to clean up the data. Radon transform or Tau-P processing is an alternative option, a last resort when other methods fail to enhance the dataset. The Tau stands for intercept time at the zero offset position. P is the slowness parameter of the ray in Snell's Law. Seismic noise is sometimes more easily removed in the Tau-P domain. A drawback is that the transform back to the TX domain is rather sensitive to errors, because the operator is not orthogonal (Trad *et al.* 2003). Furthermore, the Radon Transform suffers from loss of resolution and aliasing, arising from incompleteness of information due to limited aperture and discretization of the data or time sampling (Querne, pers. com.).

In general, multiples are bad news because inversion will treat them as primaries. Aggressive de-multiple operators, however, may cause unwanted damage to the primaries. Decisions on the correct trade-off are usually made on reflec-

tivity sections. The suppression test results may look different in the pre-stack domain. Hence, combined pre- and post-stack testing is recommendable for multiple suppression. Artefacts in the input data clearly will lead to unreliable inversion results. Multiple suppression, amplitude balancing and true amplitude processing are closely related subjects that highly influence the inversion end-results. A preserved amplitude section often looks different from a section that pleases the interpreter's eye. The ideal input to seismic inversion are of course amplitudes that are directly proportional to the subsurface reflection coefficients.

Proper data conditioning is essential for later quantitative interpretation of the inversion end results, i.e. when reservoir characterisation and lateral prediction studies are required (Da Silva *et al.*, in prep). For that matter reprocessing of the seismic dataset may prove necessary; even complete re-shoots are sometimes justified (e.g. Onderwater *et al.* 1996). The original data was processed with a special target in mind and all parameters were tuned to this objective. The later use of the same seismic dataset in pre-stack analysis was unfortunately not always foreseen. Pre-stack time migration results in better positioned seismic energy and also the velocity picking is more accurate. The current demands, made by the reservoir engineer on the quality of reliable output at all stages of the seismic processing, have increased the tasks of the geophysicist over the last decade. Detailed knowledge of



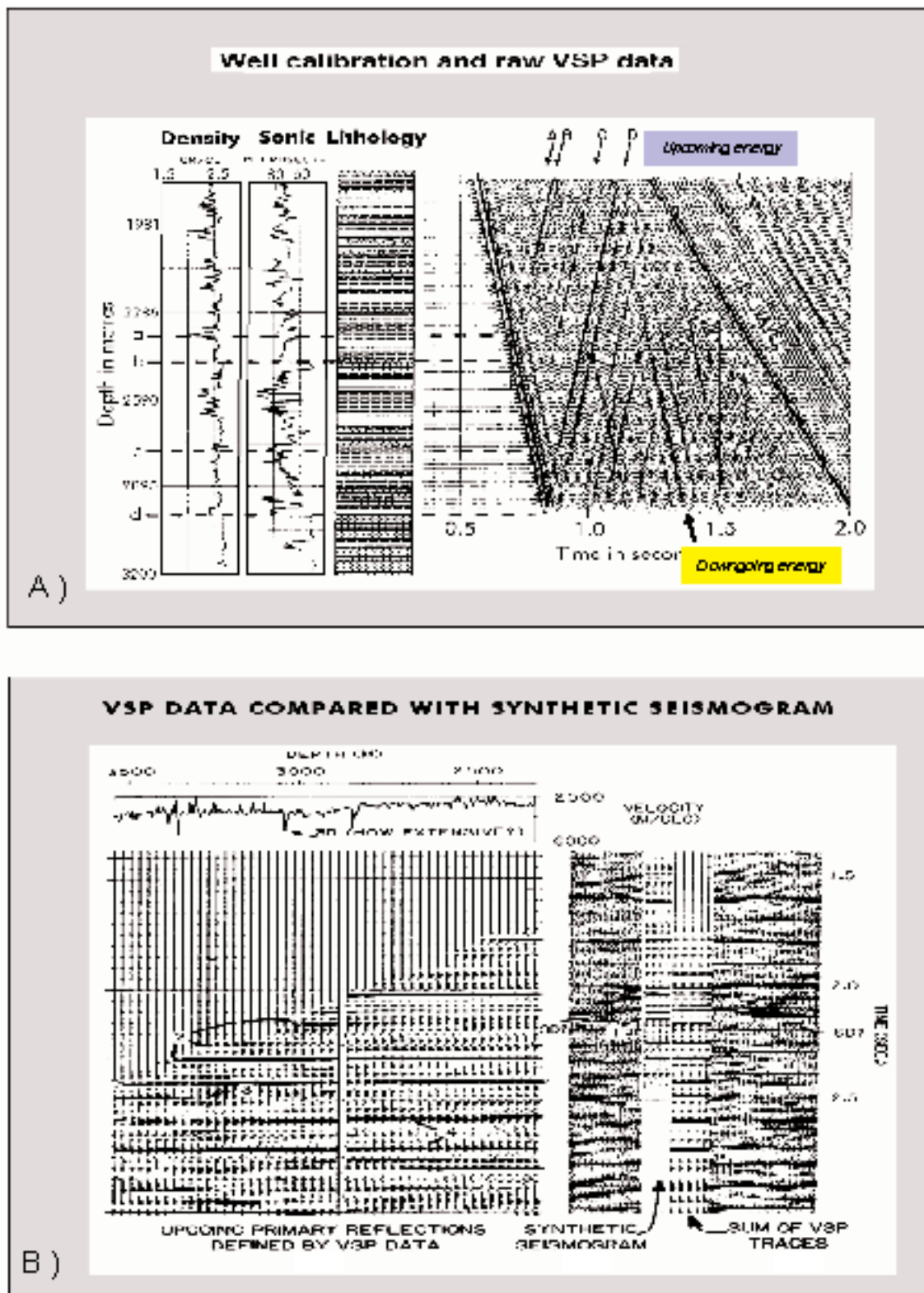


Figure 6 VSP and synthetic seismogram display for comparison of the seismic resolution. The upcoming waves are separated from the downgoing waves by F-K filtering. Alternatively the first break time can be added to each trace to line-up the upcoming energy. If it is subtracted, then the downgoing energy is horizontally lined up. The VSP trace has a frequency content that is better comparable to the surface seismic dataset. The energy around the first break time is relatively clear from multiple energy and is used in the compilation of a corridor stack (modified after Hardage 1985 and Sheriff 2002).



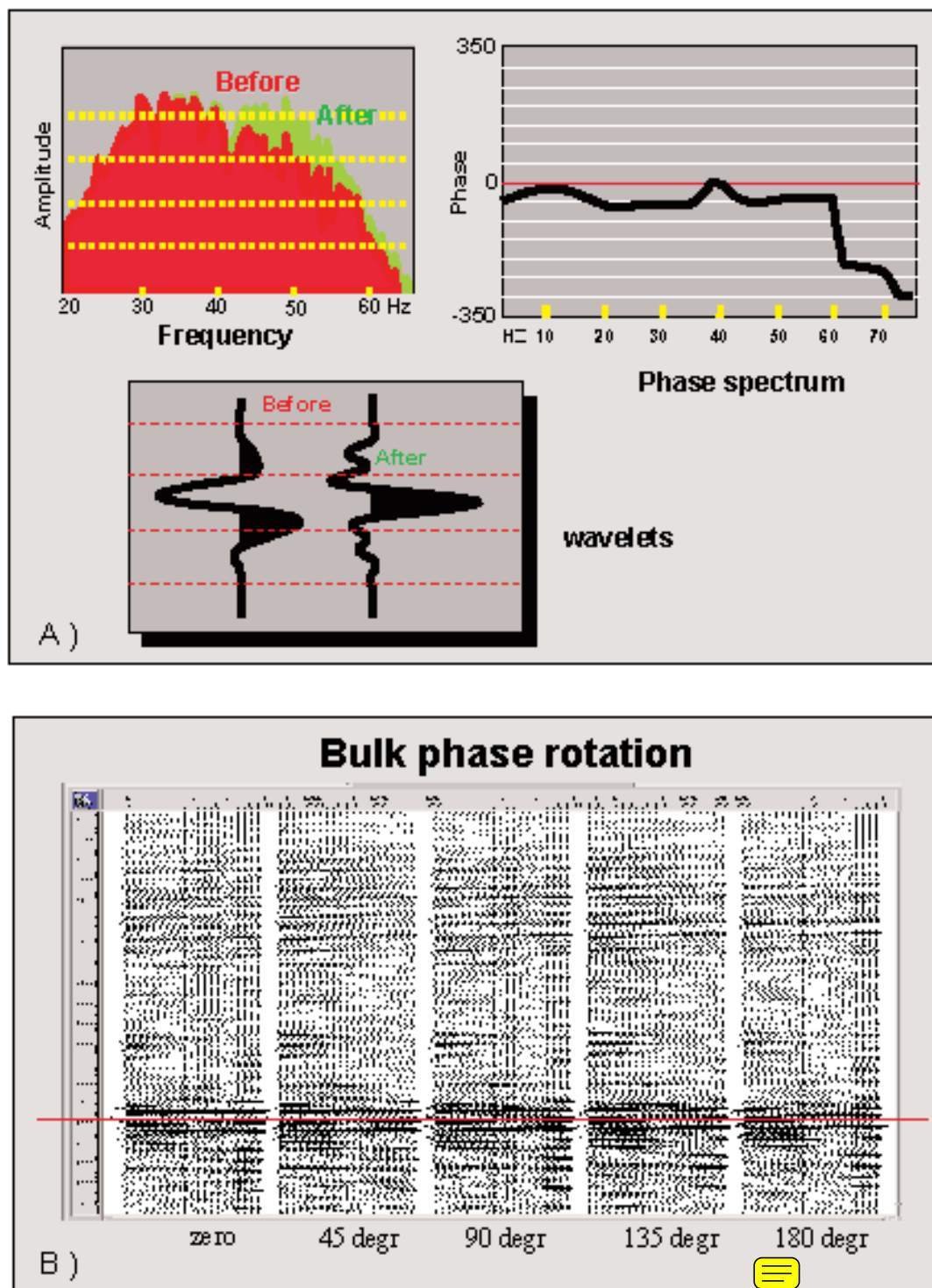


Figure 7A Amplitude and phase spectra computed for a seismic survey via the Fourier **transform**. The difference in amplitude spectra is shown before and after applying a phase correction to the seismic dataset. The bulk phase correction ensures a better match in the zone of interest. The zero-phase aspect is maintained up to 60 Hz. Two wavelets have been computed; the last one has a much better zero-phase character.

Figure 7B Bulk phase correction does leave the geometry of seismic reflections untouched, but changes their amplitudes in a systematic way. A 180° phase shift leads to an opposite polarity.

the geological model is essential to obtain sound processing products. A multi-disciplinary approach is certainly advisable to guarantee the best end result. The initiative of Comparative Analysis of Seismic Processing or CASP (Ajilani *et al.* 2003) is a step in the right direction that takes a proper balance between data quality, turnaround and costs into account.

## Wavelet extraction

### 1. Well-to-seismic tie

The well-to-seismic tie is a crucial step in seismic interpretation (a.o. White and Simm 2003). In the stratigraphic inversion scheme a comparison is made between the synthetic and the seismic trace at the well location. Several assumptions are made to derive the seismic signal or wavelet:

- Time bulk-shift of synthetic trace is correctly determined.
- Data cube is zero-phase.

The latter requirement is not always needed, but zero-phase

data will facilitate the proper identification of the position of impedance interfaces. A zero-phase dataset is characterised by a symmetrical wavelet, whereby the maximum of the central lobe corresponds with the position of the AI interface. The phase spectrum shows a near zero value for all significant frequencies. The phase spectrum is obtained when a Fourier Transform is performed (a.o. Mari *et al.* 1999). The Fourier Transform decomposes the seismic trace into individual periodic sine wave functions. Each frequency has an amplitude and phase assigned to its sine function. The results of this waveform decomposition is usually summarised in frequency spectra. The periodic waveform decomposition can be performed on the seismic trace as well as on the seismic wavelet itself.

The synthetic trace is computed from the calibrated sonic and the density logs. The sonic is converted to a velocity log for this purpose. A reflectivity trace is computed and this is convolved with the seismic wavelet to yield the synthetic trace. The sonic logs measure the transit time between two

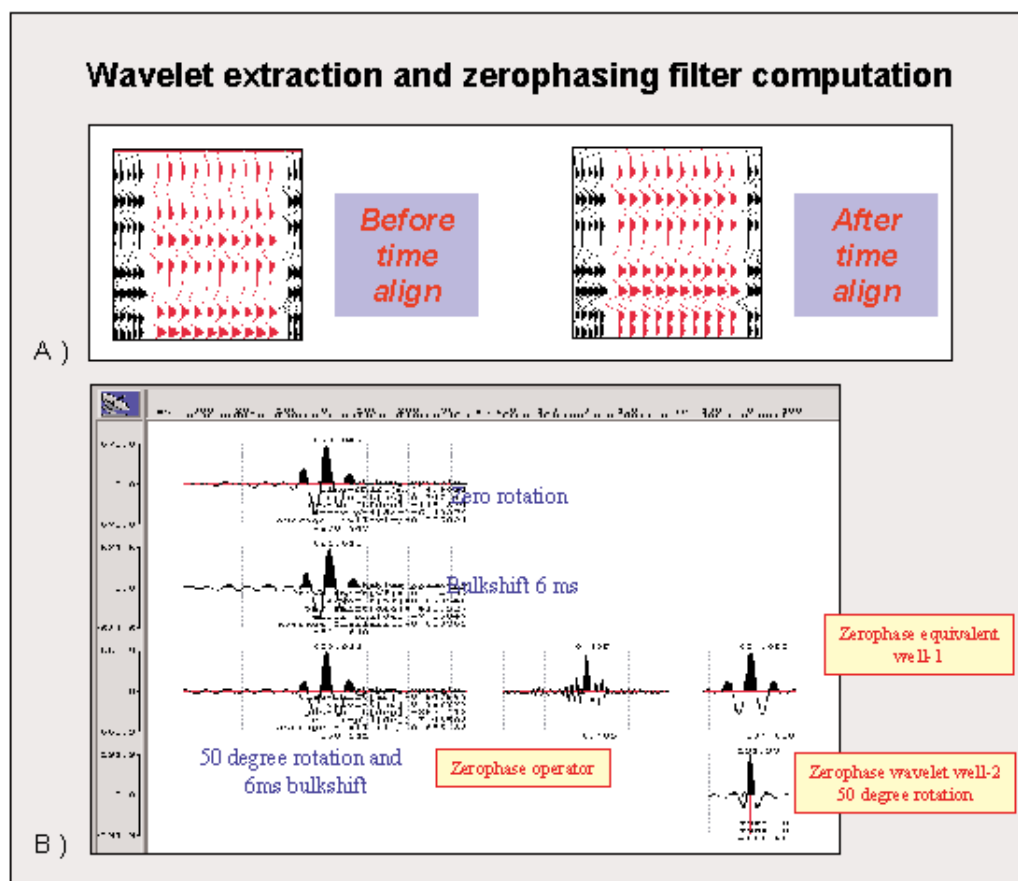


**Figure 8A** Bulk time shift is important to establish the right match between the synthetic and the seismic cube. Errors in the time shift have a major impact on the calculated phase correction in the synthetic-to-seismic well matching operation.

**Figure 8B** Computation of a zerophasing operator that converts the seismic cube within a certain time interval to its near zero-phase mode. The determination is done in a matching procedure, whereby the reflectivity trace and the seismic trace at a well location are compared. The matching operation permits the extraction of a wavelet via cross correlation procedures. Another extraction method is to design a least square error or Wiener filter. In this case the phase correction results in a sharper wavelet with less side-lobe energy.

## Synthetic traces and well match after zero-phasing

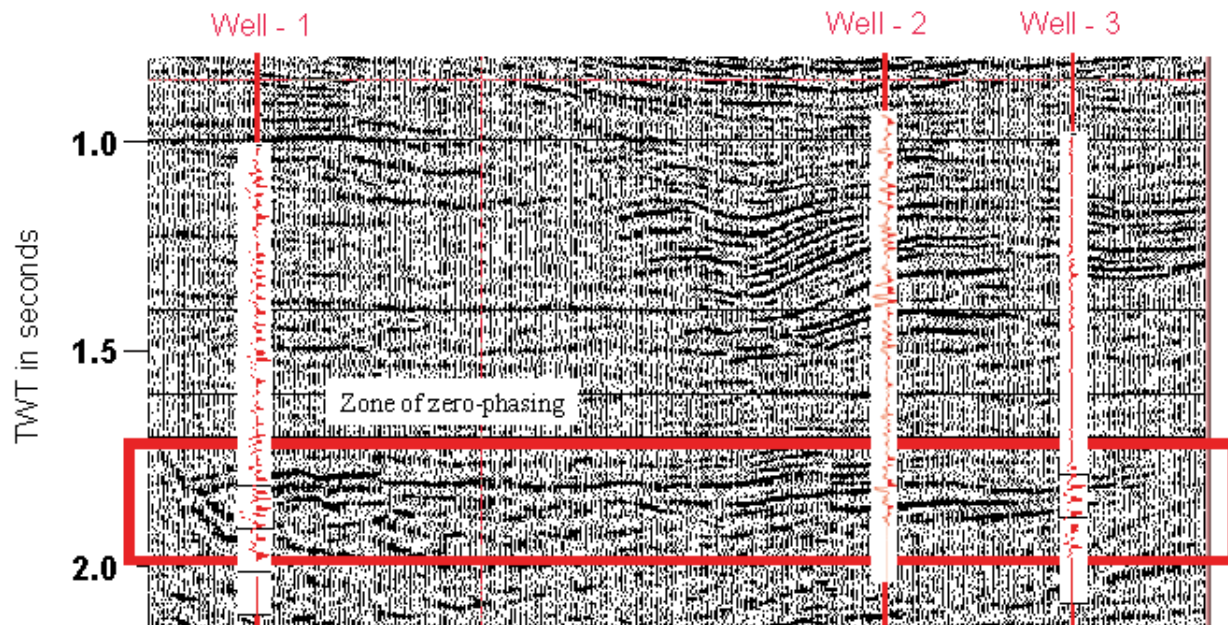
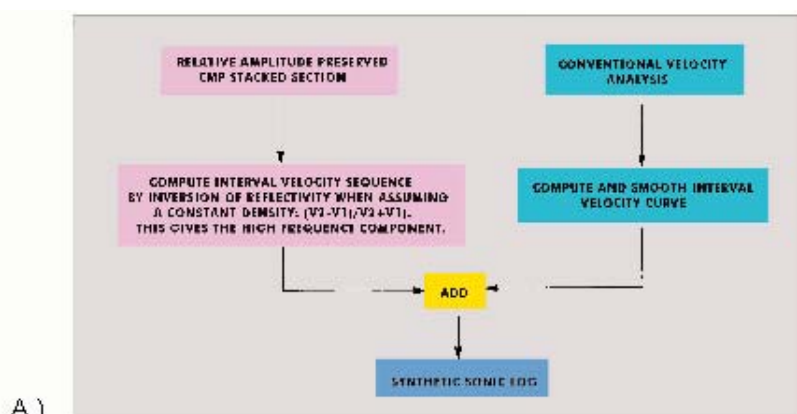


Figure 9 Match of phase rotated synthetic traces and a zero-phased seismic cube. The zero-phase condition is only valid in the red inset computation time window (courtesy Pemex).



A )

### SYNTHETIC SONIC LOG SECTION



B )

Figure 10 Integration of seismic traces is done under the assumption that the density is constant and equal to two. The high frequency variations are based on the well sonic logs and added to the seismically derived velocity trend. All traces of a seismic section are thus converted into pseudo sonic logs (modified after Yilmaz 2001).



sensors in the measuring device clamped to the borehole wall. The frequency of the sonic signal is much higher than the seismic signal. The seismic method incorporates a larger horizontal velocity component due to the acquisition geometry. Hence, slightly different velocities are measured by these two methods. The discrepancy between the sonic and seismic velocities are usually corrected with the aid of a check shot or VSP survey (cf White and Simm 2003). The discrepancy is also known as the drift of the sonic log with depth. The check shots allow time conversion of the sonic data.

The check shot survey is a simple acoustic recording of the first arrival travel time (one way time) between a shot close to the well head and various geophone positions in the well. Care should be taken not to introduce artificial steps in the calibrated sonic log at these checkshot times. This may lead to artificial reflections on the computed synthetic trace that do not exist in reality. If more than the first arrival is recorded, than a Vertical Seismic Profile (or VSP) is obtained. The VSP data requires special processing to make a direct comparison with the seismic traces possible (a.o. Veeken, in prep; Figure 6).

Sometimes the density is estimated from the P-velocity log and the following relationship is used (Gardner *et al.* 1975):

$$\text{Density} = 0.31 (\text{velocity } P_{\text{wave}})^{1/4} \quad (2)$$

The velocity is expressed in m/s and the density in g/cm<sup>3</sup>. The constant 0.31 is in fact lithology dependent and can be adjusted. Here it corresponds to sandy reservoir layers. According to Faust (1951 and 1953) the velocity can be estimated from the resistivity log:

$$V_p = 2000 (\text{resistivity} * z)^{0.16666} \quad (3)$$

The  $V_p$  is expressed in ft/s, resistivity in ohm/ft and the maximum burial depth  $z$  in feet.

A wavelet is now established by two techniques:

- Applying cross-correlation techniques between the synthetic and the seismic trace at the well location.
- Designing a shaping filter that permits transformation of the reflectivity trace into the seismic trace.

The shape of the wavelet depends very much on the time window chosen. A stable wavelet is usually derived in a maximum 1 second TWT time window. The change of the wavelet is caused by the fact that the seismic signal gets progressively distorted on its way into the earth. Moreover, poor and unreliable well logs may give rise to an erroneous wavelet and therefore quality control is a crucial issue throughout the entire processing sequence.

This wavelet is subsequently utilised to perform the seismic inversion, whereby the seismic traces are transformed into blocky seismic impedance traces. The spiked response is expressed by the limits of these blocked impedance units.

These reflectivity spikes correspond much better to meaningful geological boundaries and internal reservoir interfaces (Van Riel 2000, Veeken *et al.* 2002).

## 2. Zero-phasing and phase rotation angle

Many steps in seismic processing assume that the data are zero-phase. Zero-phase means that the phase spectrum of the seismic is flat (between 10 and 60 Hz on Figure 7A). An operator is designed for zero-phasing of the seismic sub-cube (Figure 8). The zero-phasing is normally achieved within a small time window of about 1 second TWT. If the window is selected too small, there are not enough sampling points to perform a reliable calculation. The matching procedures comprises the following steps:

- Determining and applying a bulk time shift for the well synthetic trace (Figure 8). This trace is computed from the time-converted calibrated sonic and density logs.
- Comparison of the two traces yields a seismic wavelet and a zero-phasing operator is designed.

Many times only a bulk phase rotation angle is calculated for the seismic cube (Veeken *et al.* 2002). The change in rotation angle has an influence on the shape of the wavelet, because the match between rotated seismic and the well reflectivity trace will be no longer the same. A bulk phase rotation applied to all frequencies does not alter the geometry of the seismic reflections, but influences the polarity aspect of the display (Figure 7B). The phase rotation optimises the fit between the synthetic trace and the seismic trace at the well location (Figure 9). The aim now is to design a phase rotation whereby the wavelet is zero-phase in shape. This is equal to a more symmetric wavelet, with pre-runners and post-cursors. Applying this bulk phase rotation to the dataset is in fact equivalent to the effect of a zero-phasing operator on the seismic input data. After applying the phase rotation to the seismic cube, a new matching procedure is normally started to extract the best wavelet. It is verified that the residual rotation and time bulk-shift are small (< +/-1ms and < 30 degrees). The final wavelet is computed and the actual inversion of the seismic data can now begin.

The non zero-phase aspect of the data can also be directly incorporated in the wavelet used for the inversion. The irregular shape of the non zero-phase wavelet compensates for the fact that the data are not zero-phase. Amazingly it also can take care of a part of the systematic noise (e.g. rudimentary multiple ringing).

## Various seismic inversion methods

Several methods are available to perform a seismic inversion. The approach is either deterministic or probabilistic in nature. The deterministic methods are represented by:

- Simple integration of the seismic traces.
- Sparse spike inversion.
- Coloured inversion.
- Model driven inversion.

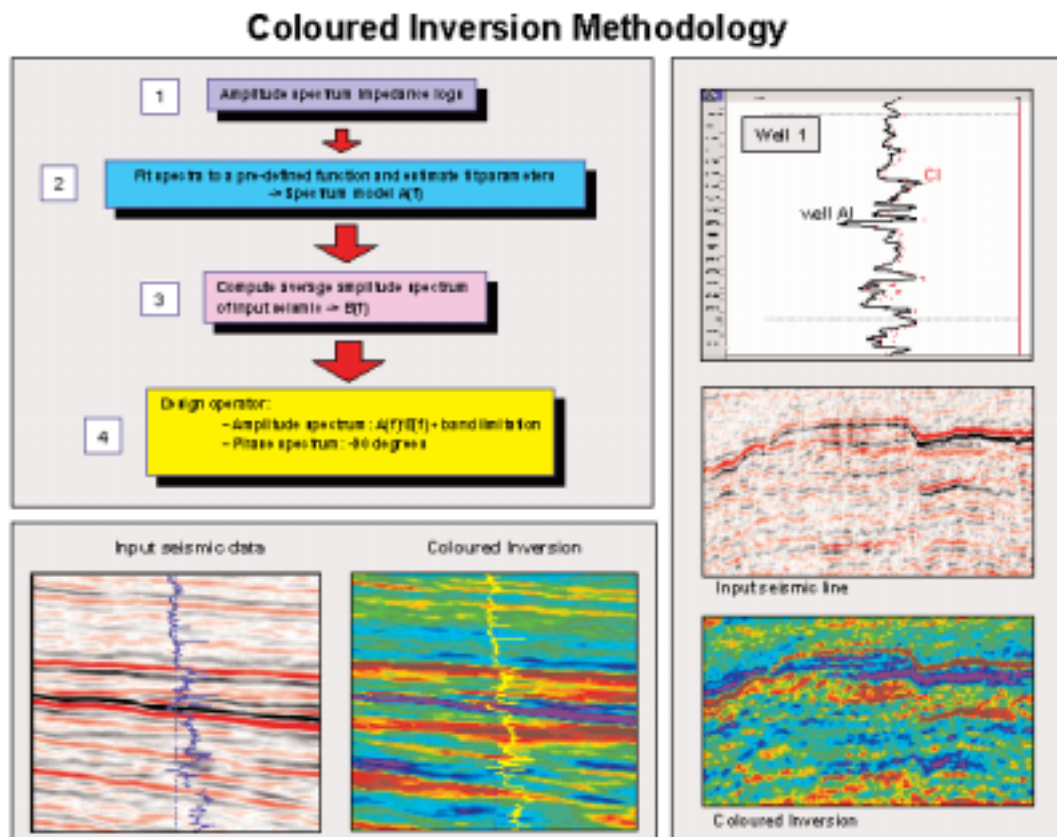


**Figure 11** Coloured inversion of seismic data exploits the frequency spectra of the logs. An average amplitude spectrum of the input seismic is computed to derive an inversion operator. This operator is applied to the seismic cube, so that its amplitudes are in better agreement with the well data. A coloured inversion example is given for seismic traces around a well. The lithological units are more easy to recognise on the coloured inversion sections. The coloured seismic inversion is a fast method, but the results are rather imprecise and only suitable for a quick look approach. For more accuracy a different inversion approach is highly advisable (courtesy CGG).

The stochastic inversion scheme uses a statistical description of the subsurface to do the inversion. Uncertainties in the input model are quantified and these are also retained in the end results.

The input of an inversion exercise consists of post-and/or pre-stack data. The pre-stack method exploits AVO effects in the dataset. As stated already, it is important that the data are as clean as possible with only a limited amount of amplitude distortion if quantitative interpretation is the objective (Da Silva *et al.*, in prep). The pre-stack data should be properly migrated.

#### Deterministic inversion

##### 1. Simple integration of the seismic traces.

Simple integration of seismic traces has been carried out in earlier years (1970-80s) to obtain reflection coefficients under the assumption that the density is constant and equal to 2.0 (Figure 10; Yilmaz 2001).

The seismically derived velocity trends are limited in their frequency contents and to compensate for this phenomenon, it is possible to construct a 'synthetic sonic log section'

(Lindseth 1979, Yilmaz 1987). A high-frequency velocity component is derived from the sonic log data in a well or from several wells. This velocity field is interpolated between the control points. A basic trend is established between the sonic log and the seismically derived velocity field; thus the high-frequency trend is approximated.

It is assumed that there is no variation in density. The seismic response is then directly translated in a vertical low-frequency velocity trend for each of the seismic traces. The high-frequency velocity component is added to this velocity trend and a pseudo sonic log trace is derived under the assumption that the density is 2.0. In this way all seismic traces are inverted to velocity changes and the inverted traces are called pseudo synthetic sonic logs. This type of trace inversion is a poor man's job that can be done better.

##### 2. Coloured inversion

The coloured inversion method is based on a special filtering technique. The amplitude spectrum of the well log in the inversion window is compared with that of the seismic

dataset (Figure 11). An operator is designed bringing the seismic amplitudes in correspondence with those seen in the well. This operator is subsequently applied to the whole seismic cube (Lancaster and Whitcombe 2000). A crossplot is made between the amplitude and the logarithm of the frequency to compute the operator. A linear fit is performed to calculate an exponential function  $f^\alpha$  and this serves as a shaping filter (cf Walden and Hosken 1985, Velzeboer 1981). This filter trans-

forms the seismic trace into an assumed acoustic impedance equivalent. The assumption is made that the seismic input cube is zero-phase, which is hardly ever the case. Again, it is a quick and rather imprecise inversion method.

### 3. Sparse spike inversion

In this method the seismic trace is simulated from a minimum number of AI interfaces (or reflectivity spikes) that will

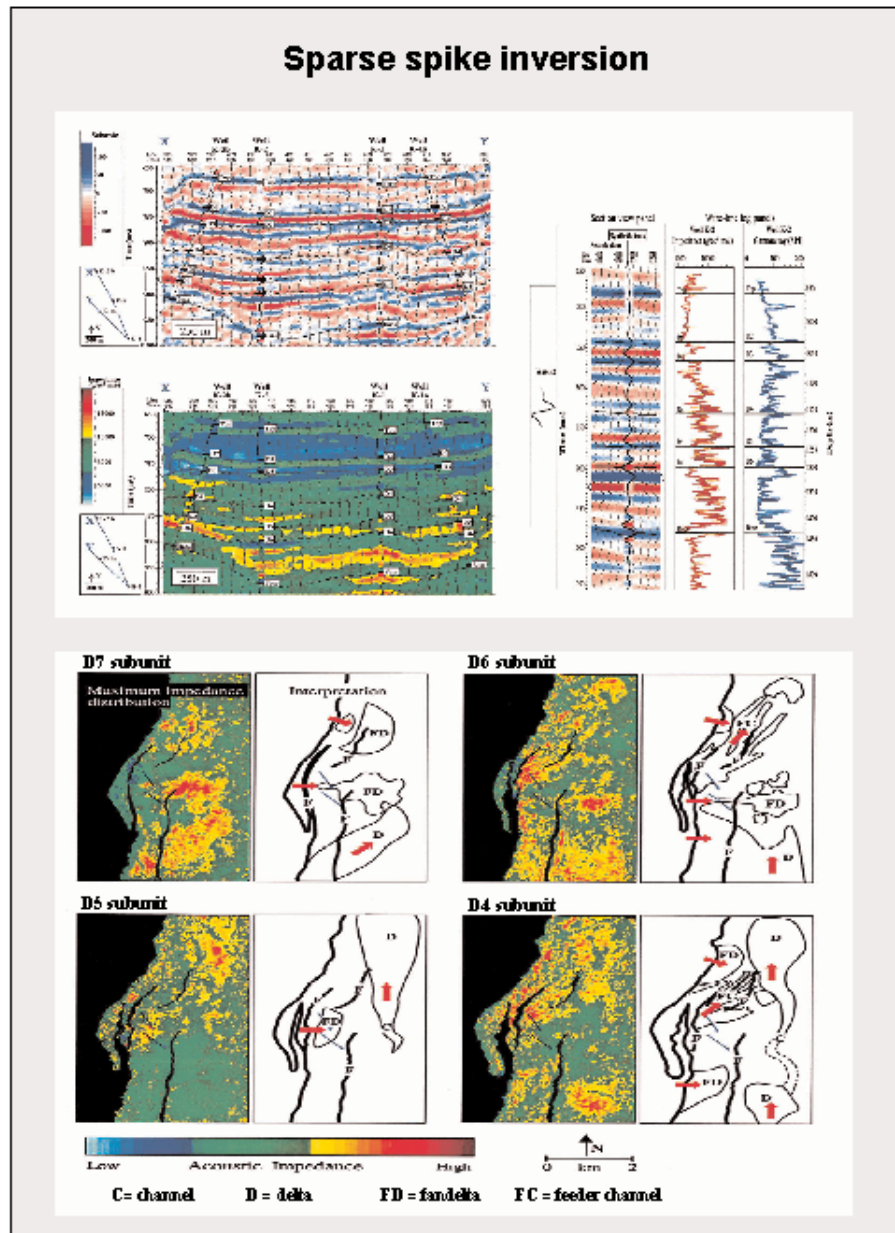


Figure 12 Sparse spike inversion uses a minimum number of acoustic impedance interfaces to model the subsurface reflectivity. The algorithm was initially working on a trace by trace basis that caused some instability in the inversion results. A 3D approach is now adopted and further constraints for the solution are provided by the low frequency variation observed by the well control. It is interesting to note that the wavelet used in this study is not zero-phase (modified after Ronghe and Surarat 2002).



reproduce the real seismic response when convolved with the wavelet. Amplitude, time position and number of the reflectivity spikes are not always realistic, i.e. not necessarily corresponding to the geological constraints. If a starting model is not available, the spikes might be placed in an unrealistic way and still generate a synthetic that highly resembles the real seismic trace. The recursive method uses a feedback mechanism to generate a more satisfactory output.

The inversion algorithm was initially only working on a trace-by-trace basis, but now a multi-trace approach is implemented. The inversion solution may vary considerably from trace to trace, thus making the reliability of the output weaker. A low frequency AI variation trend can be imported to obtain more appropriate results and get a better convergence for the found solutions from trace to trace. The constrained option uses a low frequency model as a guide (Figure 12). The low frequency variation is estimated from blocked well logs and this gives much better results (e.g. Ronghe and Surarat, 2002). The inversion replaces the seis-

mic trace by a pseudo acoustic impedance trace at each CDP position (Pendrel and Van Riel 1998). The sparse spike assumption implies, however, that a thin bed geometry will not always be mimicked in the most optimal way.

The zero-phase requirement can be circumvented by choosing a compound wavelet for the inversion, thus compensating the non zero-phase aspect of the input data (Figure 12). The multi-trace approach results in a much better stability of the computed solution. Sophisticated model-driven sparse spike inversion give more realistic output. Many times the interpreter gets away with the sparse spike approximation, but in the majority of cases yet a better solution is needed.

#### 4. Model-driven inversion

In this method a simple initial AI model is perturbed and a synthetic trace is computed using the seismic wavelet. The difference between this synthetic trace and the real seismic trace is determined (cf. Cook and Sneider 1983, Fabre *et al.* 1989, Gluck *et al.* 1997). The AI model with a very small dif-

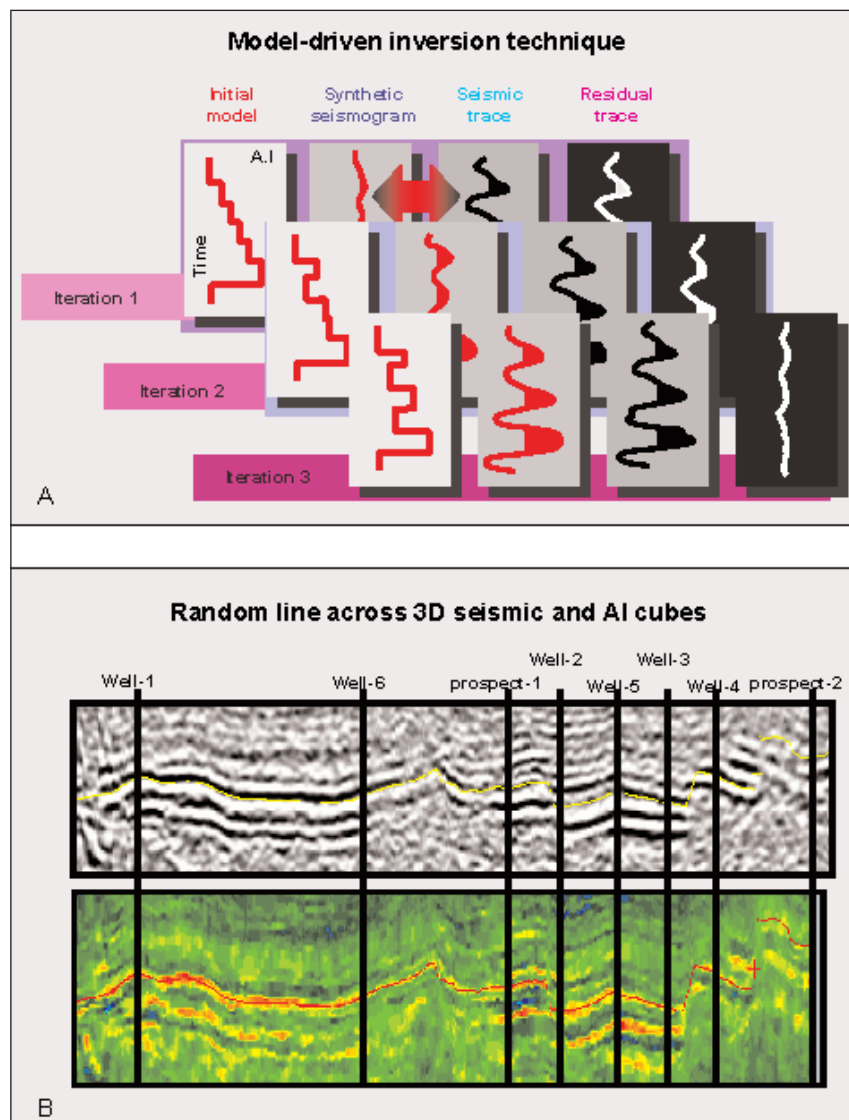


**Figure 13A** Model driven seismic inversion method. A simplistic initial stratigraphic model (macro and micro) is convolved with the wavelet to obtain a synthetic response that can be compared with the actual seismic trace. The macro layers are formed by the mapped TWT horizons. Microlayers are automatically introduced into the macro-model to define a grid cell volume – based on inline, crossline and microlayer – for storing constant AI values. The AI model is perturbed, whereby the difference between inverted trace and the seismic trace is reduced until a small threshold value is reached (Veeken *et al.* 2002).

**Figure 13B** Arbitrary seismic line through various wells. The inversion result below shows anomalous layers with a decrease in acoustic impedance. Red represents high and blue the lower AI values. Computational constraints compel that the macro layers are continuous over the survey area and interpolation has been done in the fault zone polygons to fill the gaps in the grids. Inversion results in the fault zones are therefore physically meaningless (courtesy Pemex).

ference is retained as solution (Figure 13). A simulated annealing technique using a Monte Carlo procedure is applied (Goffe *et al.* 1994, Duboz *et al.* 1998). This technique shows a resemblance to the growth of crystals in a cooling volcanic melt (Ma 2003). It starts with a reflectivity model  $M_0$  and computes the difference with the seismic input data after convolution with a wavelet. The model is perturbed and a new model  $M_N$  is simulated, for which the same difference is established. The two differences are compared and if the misfit for  $f(M_N)$  is smaller than that for  $M_0$ , then the  $M_N$  model is unconditionally accepted. If not, then the  $M_N$  model is accepted but with a probability  $P = \exp(-f(M_N) - f(M_0)/T)$ , whereby  $T$  is a control parameter (acceptance temperature). This acceptance rule is known as the Metropolis criterion (Metropolis *et al.* 1953). The process is repeated a large number of times, until a very small residual difference (or threshold value) is found. Computation of cost functions enables the determination of a real regional minimum for these differences.

The initial AI model is made up of macro-layers defined by the shape of the seismic mapped horizons. Micro-layers are automatically introduced in this macro model. It provides a stratigraphic grid cell volume together with the inline and crossline subdivision for storing constant AI values. The use of micro-layers ensures that an adequate number of

spikes is utilised in the modelling. Normally these layers are 5-7 ms TWT thick. Several parameters can be set for use in the inversion algorithm and corridors define boundaries for the amount of variation (Figure 14). The method is robust and a real 3D inversion algorithm is applied (Coulon *et al.* 2000, Veeken *et al.* 2002). The latter is important for the stability of the retained solution.

The model-driven inversion gives satisfactory results, even when well control is limited and the seismic quality is rather poor. It is also possible to derive a wavelet straight from the seismics by auto-correlation techniques. Even non zero-phase wavelets can be utilised as described earlier on. Well control is not always completely honoured by this method, but a great advantage is that the seismic data are the guide for the inversion. The averaging effect of the 3D approach gives rise to small discrepancies at the well locations that are in fact quite acceptable.

Another model-driven method (Invermod) makes use of Principal Component Analysis (PCA, Helland-Hansen *et al.* 1997). The principal component method computes a standard response from which the input can be generated by applying specific weighting factors. These weighting factors are extrapolated over the study area to allow predictions outside the control points. The inversion needs an a-priori starting model. The structural frame of the model is based on the

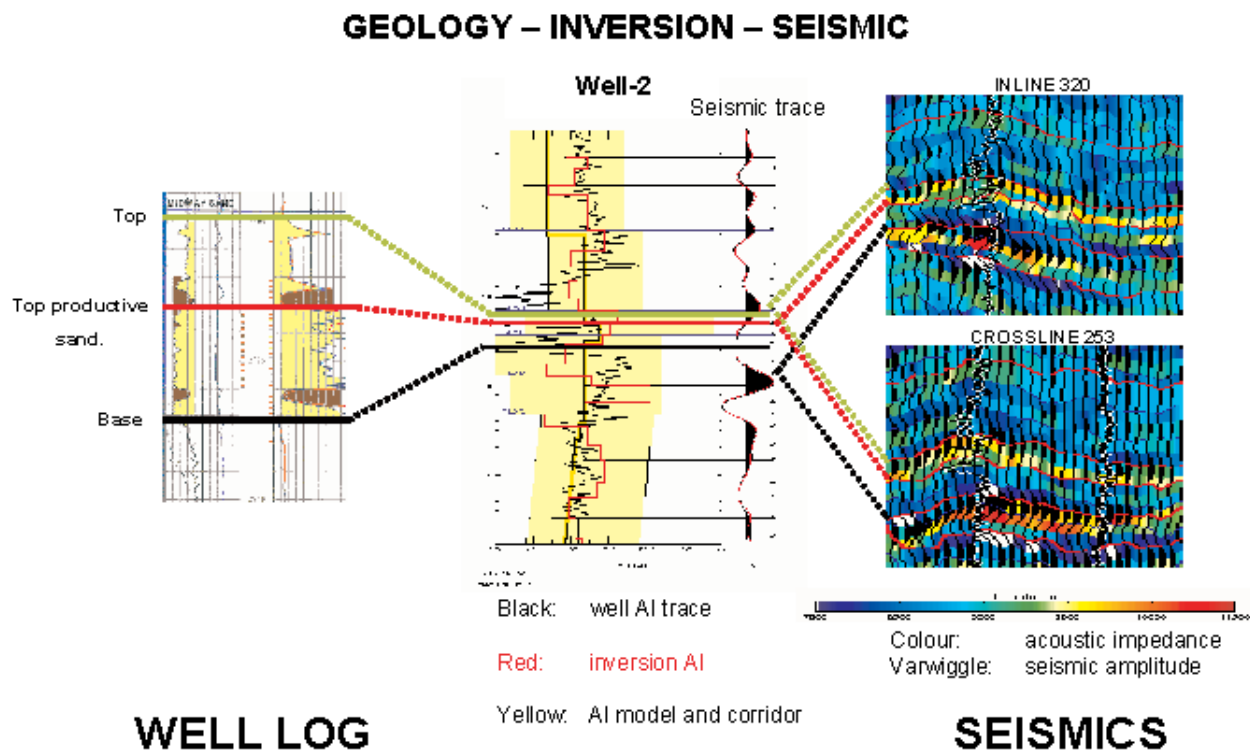


**Figure 14** Comparison of well data and inversion results. On the right hand side the seismic wiggles are overlying the coloured AI values. Lateral changes in AI are of interest to determine fluid fill in reservoir sands. Inversion may even lead to detection of the behaviour of thin beds beyond seismic resolution. Subtle changes in seismic loop shape (doublets) are exploited in this manner.

## Stochastic inversion

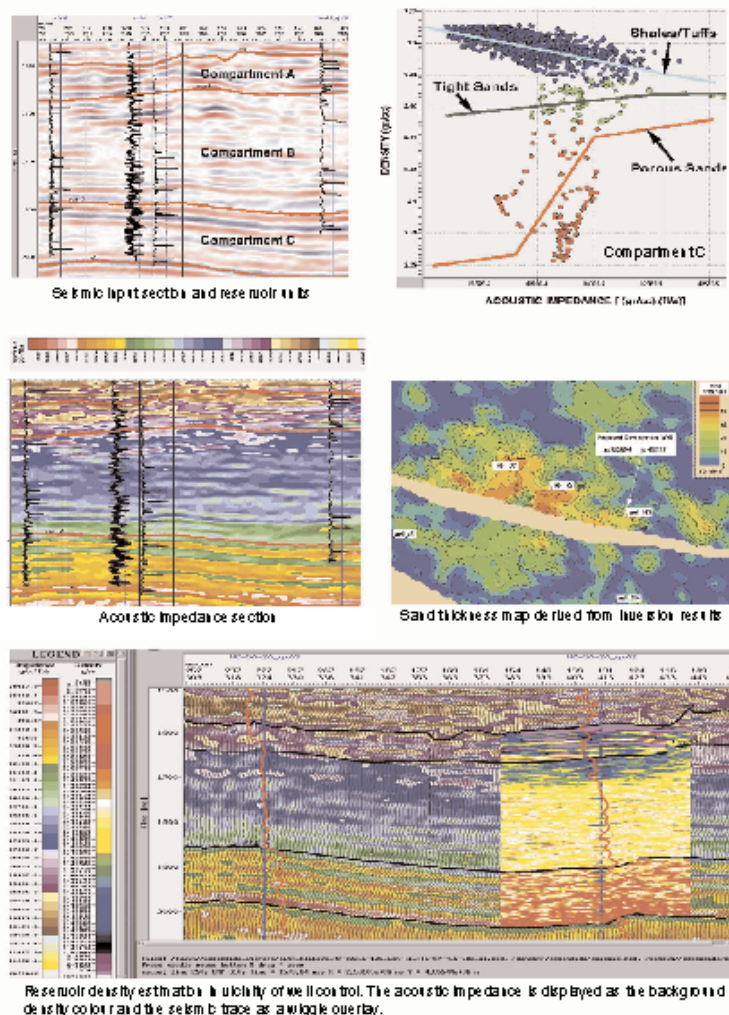


Figure 15 Probabilistic inversion uses quantification of uncertainties attached to the inversion input data. Probability density functions (PDF) are defined and an earth model is simulated, which is perturbed to minimise the discrepancy between the modelled and measured seismic data. The inversion results are summarised in P10, P50 and P90 maps. Individual realisations are often dangerous to interpret. It is more useful to determine stable areas in the suite of simulations. The confidence for the reliability of the inversion results in these zones is increased. The statistical variability in geometry of geological bodies is taken into account in this inversion scheme (modified after Torres-Verdin *et al.* 1999).

shape of the mapped time horizons. The initial model, with the separate velocity and density distribution, is built by PCA from the well log data. Weighting factors for the standard log response in the studied area are determined via a linear interpolation. The results of the convolution with the seismic wavelet are compared with the seismic traces and the Vp-rho models are perturbed to reduce the discrepancy. The velocity and density are hereby modelled separately, which can be tricky sometimes.

### Stochastic inversion

Geostatistics are used to build complete subsurface reservoir models or realisations. Simulation is done on a local level as well as globally on the totality of the generated model (Haas and Dubrule 1994, Dubrule 2003). All models honour the well data. The simulation can be based on variations per pixel or objects. The architecture of reservoirs is usually classified in various ways (Weber and Van Geuns 1990) and this

classification of the wells helps in selecting the simulation approach. Probability Density Functions (PDFs) are established for each grid point and these are utilised to perform a random simulation (Torres-Verdin *et al.* 1999; Van der Laan and Pendrel 2001). The input for the PDF determination comes from: well logs, spatial properties (variograms) and lithological distributions (Figure 15). The stochastic algorithm calculates for each simulation a synthetic trace, compares it with the real seismic trace, and accepts or rejects it. A simulated annealing process is utilised. The number of solutions is reduced in this way and probability maps are produced to assess the amount of uncertainty. The retained simulations are examined on their variance. If they closely resemble each other, then the prediction is rather good and the confidence in the scenarios is increased.

The earth models show a high resolution variability comparable to that found in the wells. The proposed variability is clearly beyond seismic resolution. When production data



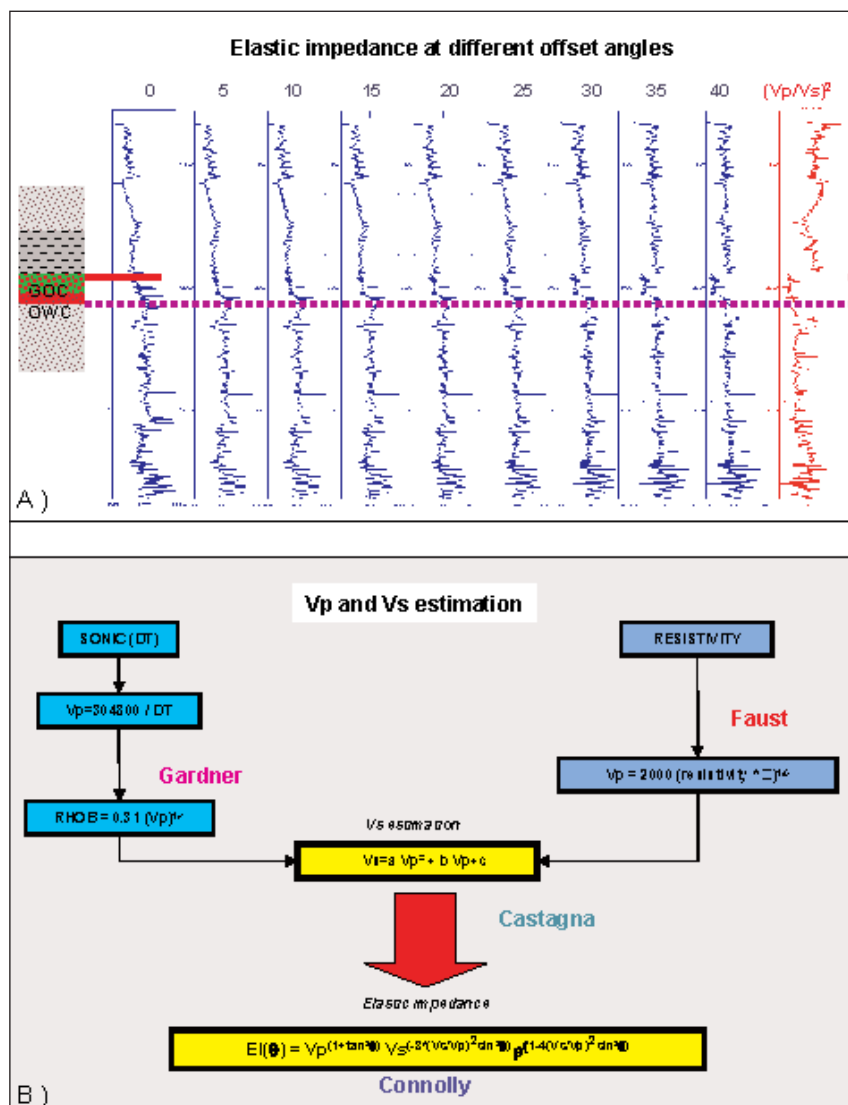


Figure 16A Elastic impedance logs computed for the various offset angles. The top of the gas reservoir is well expressed at the larger incidence angles. The  $V_p/V_s$  ratio also shows a remarkable break at this contact.

Figure 16B Estimation of  $V_p$  and  $V_s$  velocities. A polynomial trend is proposed by Castagna (1993) that is adaptable to sandy, silty, shaley and carbonate reservoirs. These estimations are needed to calculate the Elastic Impedance attribute at the different incidence angles (Connolly 1999).

are integrated in the modelling constraints, then the value of the simulated model is increased accordingly. Production history matching and pressure monitoring gives an indication for the connected reservoir volume and its permeability.

A probability volume is generated for grid points with porosities above 10%, using the simulation histograms. Subsequently geobodies are outlined, where the probability is for instance above 70% for the porosity to be higher than 10%. As more wells are drilled in the petroleum system, the best matched simulations are retained to further refine the predictions (Sylta and Krokstad 2003).

The drawback of the method is that the interpreter has to quantify the uncertainties in a realistic way. This a tedious and somewhat precarious task. Areas without proper well control are difficult to predict and certain assumptions have to be made. There is a cumulative increase in prediction error. Another problem is selection of a suitable presentation of the results. Normally only the P10, P50 and P90 cases are retained in the output and the rest of the realisations are ignored. These

P10-P90 maps can be somewhat misleading as the outcome of an individual simulation is not always realistic, e.g. very rapid changes in geological style that are an artefact of the working method. It is better to use maps that are some sort of an average and concentrate on the areas that are rather stable in several simulations. The predictive value of the simulation is strongly reduced in areas with great variability in outcome of the realisations. The averaging procedure has, however, a negative effect on the high resolution aspect of the proposed solution.

#### Pre-stack inversion

##### Elastic inversion (EI)

The method exploits AVO effects in the pre-stack domain and uses  $V_p$ ,  $V_s$  and density information. Shear waves may yield valuable information on the lithological distribution (Pendrel *et al.* 1998). The S-waves mainly interact with the rock frame work, whereas the P-waves are influenced by the porefill and rock matrix. The  $V_s$  is often estimated in wells using the Castagna formula (Castagna and Backus 1993, Figure 16).

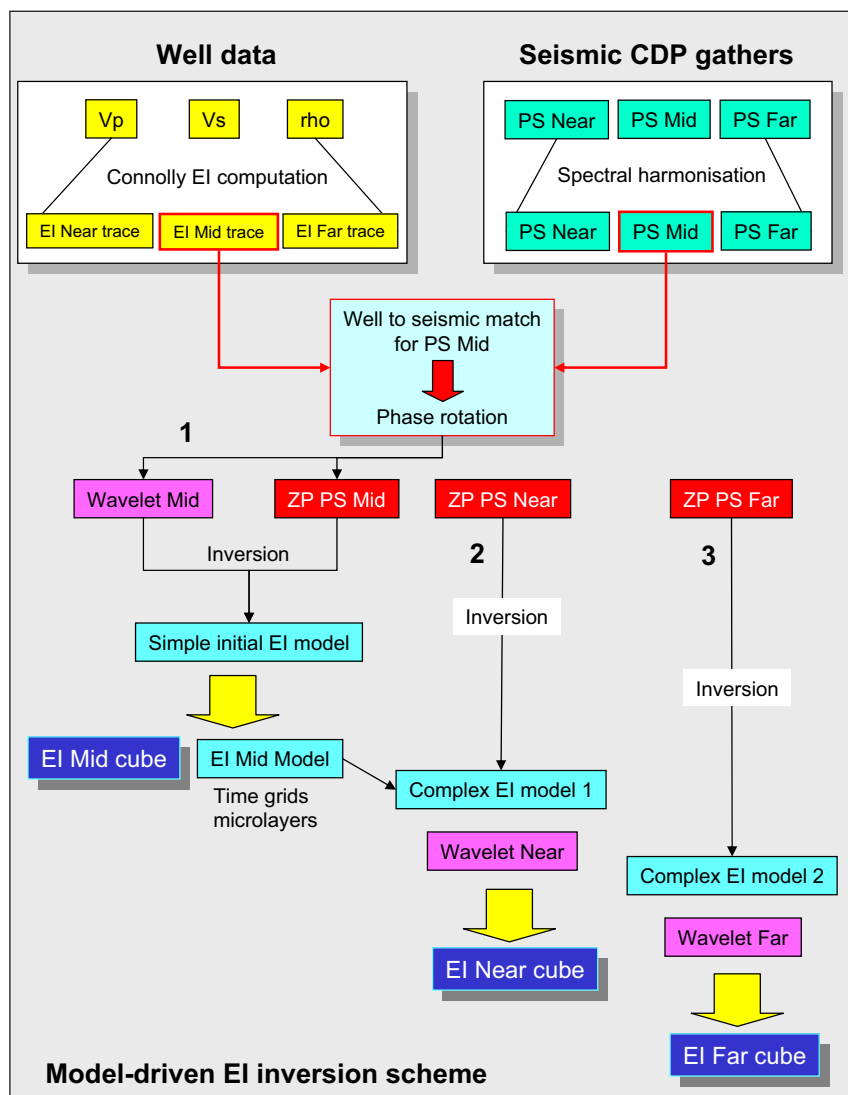


**Figure 17** A flow chart for elastic inversion processing. The procedure is rather complex and time consuming. PS stands for partial stacks and ZP for zerophased seismic volume. The 'EI 1 trace' is the EI response computed from the well data at the centre position of Near offset range; the EI 2 and 3 traces are corresponding with the Mid and Far. The procedure gives access to rock physical parameters like the attributes  $R_p$ ,  $R_s$ ,  $I_p$ ,  $I_s$ ,  $V_p/V_s$ ,  $\rho_{\text{mu}}$  and  $\rho_{\text{lambda}}$ .

The full Zoeppritz equations give a description of the amplitude behaviour of reflector with offset (Zoeppritz 1919). These equations are tedious to work with and therefore an approximation is introduced, valid under certain conditions (e.g. Aki and Richards 1980; Shuey 1985). The Shuey equation gives an approximation of the Zoeppritz reflectivity that is good up to 30-35° incidence angle. The assumption is made that  $V_p$  is approximately twice  $V_s$  and the higher terms are dropped due to the 30° angle of incidence condition. When working with pre-stack data, it is necessary to make a better estimation by taking into account the difference in  $V_p$  and  $V_s$ . This is done by adopting a so-called elastic approach. Connolly (1999) introduced the concept of Elastic Impedance. He defined a function  $F(\theta)$  that is incidence angle dependent and related to the P-wave reflectivity in the following manner:

$$R(\theta) = (F(t_i) - F(t_{i-1})) / (F(t_i) + F(t_{i-1})) \quad (4)$$

This function  $F(\theta)$  is now called the Elastic Impedance, in analogue to the acoustic impedance concept. The angle dependant P-wave reflectivity is also approximated by the well known simplified description of the Zoeppritz equations:

$$R(\theta) = A + B \sin^2 \theta + C \sin^2 \theta \tan^2 \theta \quad (5)$$

$$\begin{aligned} A &= 0.5 \left( \Delta V_p / V_p + \Delta \rho / \rho \right) \\ B &= 0.5 \left( \Delta V_p / V_p \right) - 4 \left( V_s / V_p \right)^2 \left( \Delta V_s / V_s \right) - 2 \left( V_s / V_p \right)^2 \left( \Delta \rho / \rho \right) \\ C &= 0.5 \left( \Delta V_p / V_p \right) \end{aligned}$$

$$\begin{aligned} \Delta V_p &= V_{p2} - V_{p1} \\ V_p &= (V_{p1} + V_{p2}) / 2 \end{aligned}$$

Combining the two expressions (4) and (5) results in the Elastic Impedance being equal to:

$$EI_{\theta} = V_p^2 [1 + \tan^2 \theta] - V_s^2 [3K \sin^2 \theta] - \rho [1 - 4K \sin^2 \theta] \quad (6)$$

Here  $K$  is a constant, that is taken to be equal to the average of  $(V_s/V_p)^2$ .  $V_p$  and  $V_s$  are expressed in m/s and the density in  $\text{gr/cm}^3$ . This type of EI computation is performed on pre-stack gathers and takes into account the changes in  $V_p$ ,  $V_s$  and density as well as AVO effects. The approach is accurate for small to moderate impedance changes. Dropping the third term in the Shuey equation in formula (5) - which is less accurate, but faster - is equivalent to replace the  $\tan^2 \theta$  by  $\sin^2 \theta$  in the Connolly equation (6).

$$EI_{\theta} = V_p^2 [1 + \sin^2 \theta] - V_s^2 [3K \sin^2 \theta] - \rho [1 - 4K \sin^2 \theta] \quad (7)$$

There are some assumptions that need to be fulfilled for this formula (7) to be correct:

- Two term NMO approximation is correct.
- Dix's velocities are often required in the raytracing going from the offset to the angle of incidence domain. Dix's equation (Dix 1955) is valid for the following situation:
  - A layer cake geometry.
  - Offset is smaller than the depth of the reflector.
- Angle of incidence  $\theta$  is smaller than 30-35°, so that the Shuey approximation is correct (Shuey 1985).
- Transverse isotropic medium.
- Correctly balanced pre-stack amplitudes.
- Amplitudes are proportional to  $\sin^2 \theta$ .

The last point implies taking out the acquisition imprint by

### Simplified elastic impedance

Elastic impedance definition by Connolly (1999):

$$EI_{\theta} = V_p^2 (\sin^2 \theta) V_s^2 (4K \sin^2 \theta) - \rho (1 - 4K \sin^2 \theta)$$

Assumption  $\tan^2 \theta = \sin^2 \theta$  means dropping 3rd term in Shuey approximation:

$$EI_{\theta} = V_p^2 (\sin^2 \theta) V_s^2 (4K \sin^2 \theta) - \rho (1 - 4K \sin^2 \theta) \quad \text{and} \quad I_p = \rho V_p$$

Take the logarithm of both sides and this allows to get rid of exponential notation:

$$\begin{aligned} \ln EI_{\theta} &= \ln [V_p^2 (\sin^2 \theta) V_s^2 (4K \sin^2 \theta) - \rho (1 - 4K \sin^2 \theta)] \\ &= \ln (I_p^2) + \ln [(\sin^2 \theta) V_s^2 (4K \sin^2 \theta) - \rho (1 - 4K \sin^2 \theta)] \\ &= \ln (I_p^2) + \sin^2 \theta \ln [V_p^2 V_s^2 (4K) - \rho (1 - 4K)] \end{aligned}$$

Assumption  $K = (V_s/V_p)^2 = 0.25$ , also known as a simplified elastic impedance.

$$\begin{aligned} \ln EI_{\theta} &= \ln (I_p^2) + \sin^2 \theta \ln [V_p^2 V_s^2 (2) - \rho (1 - 1)] \\ &= \ln (I_p^2) + \sin^2 \theta \ln (V_p^2 V_s^2 (2) (1/\rho)) \\ &= \ln (I_p^2) + \sin^2 \theta \ln [(V_p^2/V_s^2) (1/\rho V_p)] \\ &= \ln (I_p^2) + \sin^2 \theta [\ln (V_p^2/V_s^2) - \ln (\rho V_p)] \end{aligned}$$

$$\ln EI_{\theta} = \ln (I_p^2) + \sin^2 \theta [2 \ln (V_p/V_s) - \ln (\rho V_p)]$$

**Figure 18** The Elastic Impedance approximation as introduced by Connolly (1999). The logarithmic simplification is done under the assumption that  $K = 0.25$ . The main advantage is that the logarithmic EI representation avoids an awkward exponential notation.

making the necessary source and cable corrections, spherical divergence correction, static and topographic corrections, prestack time migration, multiple and noise suppression, DMO, NMO and residual NMO in order to get the best migrated stack section. The amplitude should preserve its proportional aspect to the original subsurface acoustic impedance contrasts or reflection coefficients. Visual inspection and quality control tests play a key role in securing that this objective is optimally achieved.

The benefits of the elastic impedance calculations are clearly demonstrated by Figure 16. It can be easily seen that the larger offset angles give a better discrimination at the top of the gas reservoir. Also the  $V_p/V_s$  ratio shows a distinct break at this interface. The  $EI_0$  is corresponding to the acoustic impedance  $AI (= \rho V_p)$ . If  $K = 0.25$  then the  $EI_{90} = (V_p/V_s)^2$ .

The EI seismic attribute is the basis for performing an elastic inversion similar to conventional acoustic inversion processing. In acoustic impedance inversion, a wavelet (shaping filter or cross-correlation techniques) is established between the AI trace from the well and the recorded seismic trace. In the elastic inversion, wavelets are derived for different incidence angle traces of  $EI_{(\theta)}$  and the corresponding migrated partial stack trace. A schematic EI workflow is presented in Figure 17. The diagram is rather complex and it reflects the amount of effort needed to get to the goal.

There are other formulae to approximate the EI, e.g. logarithmic approach or also a less common non-linear function (Tarantola 1984, 1986; Pica *et al.* 1990). The logarithmic function avoids tedious exponential descriptions and is valid under the condition that  $K = 0.25$  (Figure 18):

$$\ln(EI_{\theta}) = \ln(I_p^2) + (2 \ln(V_p/V_s) - \ln(I_p)) \sin^2 \theta \quad (8)$$

whereby  $I_p = \rho V_p$ .

All these formulae have their own assumptions and validity range. It means that the elastic inversion results are often only usable in a qualitative way, as the absolute value of the inversion is not necessarily correct. For quantitative interpretation more processing efforts are needed, like exploiting the full set of Zoeppritz equations.

The far offsets of these EI cubes give detailed information on the fluid contents (Figure 19). Attributes like  $R_p$ ,  $R_s$ ,  $I_p$ ,  $I_s$ ,  $V_p/V_s$ ,  $\rho$  and  $\lambda$  are easily calculated. The  $\rho$  and  $\lambda$  (cf Goodway *et al.* 1997) are derived from the following expressions:

$$\rho = I_s^2 \quad (9)$$

$$\lambda = I_p^2 - 2I_s^2 \quad (10)$$

The  $\mu$  ( $\mu$ ) and  $\lambda$  ( $\lambda$ ) are known as the Lamé's constants.  $\mu$  is the rigidity factor. The  $\lambda$  parameter is the incompressibility and contains the fluid information. Note that it is not possible to get access to the density and veloci-



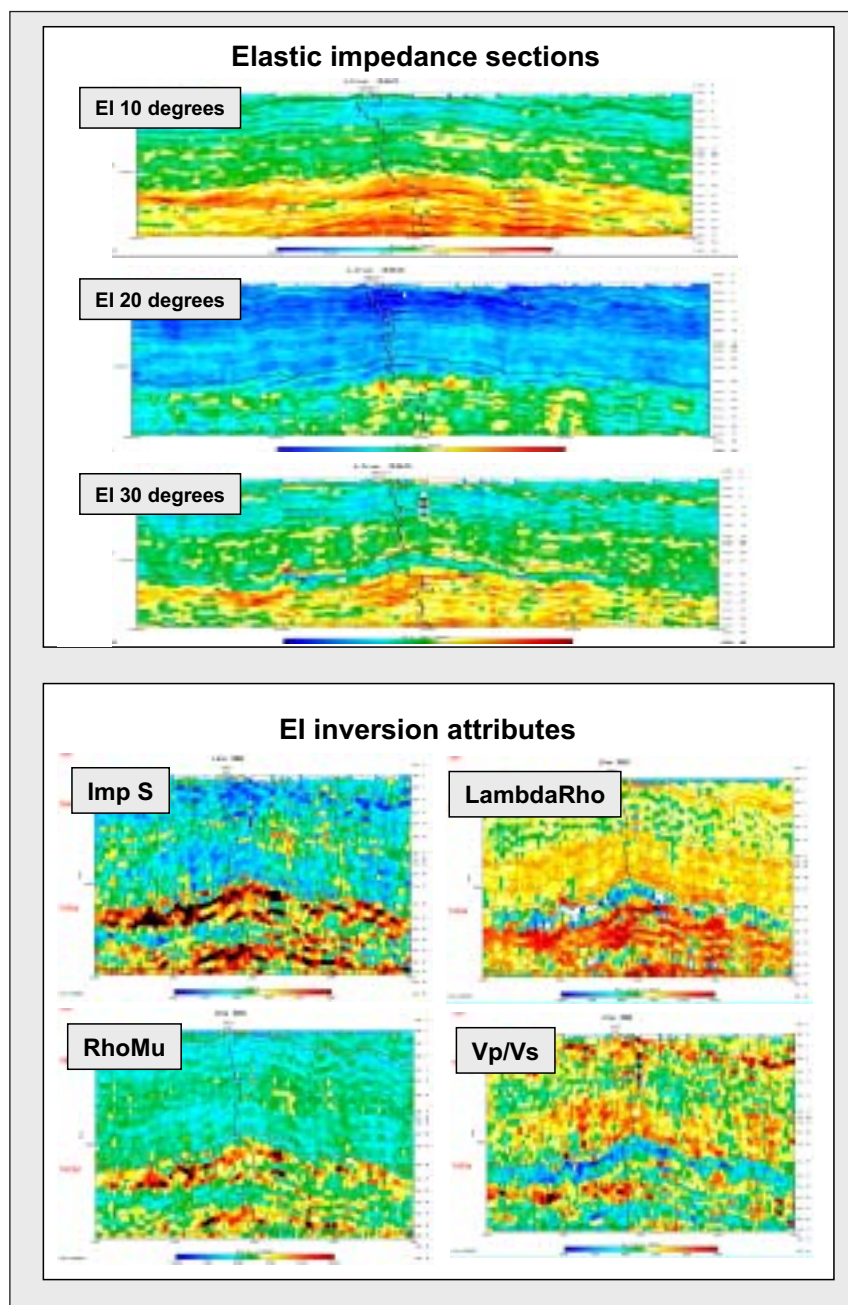


**Figure 19** The integrated approach of an elastic inversion incorporates the AVO effect on the traces of the migrated CDP gather and uses Vp and Vs information. Various angle dependent EI cubes and other seismic attributes are examined on anomalies that may correspond to lithology, porosity or fluid changes. The elastic inversion yields several seismic reservoir attributes. Crossplots demonstrate their correlation with porefill changes.

ty values directly for each separate layer via an inversion scheme. It is always necessary to make an estimation of their individual contribution to the total change in impedance of the various layers later on.

The calculated attributes are studied in detail and the attention is usually focused on anomalies. Well plots in zones of interest are utilised to carry out quantitative interpretation and to perform reservoir parameter predictions. These parameters can also be obtained via AVO analysis, but that calculation is less reliable (Cambois 2000).

## 2. Simultaneous inversion

Simultaneous inversion is calculating synthetic gathers from

perturbed P- and S-reflectivity models. The method is described in detail by Ma (2002) and his article serves here as a guide. The approach is basically model-driven. The inversion is achieved by applying a simulated annealing technique (Ma 2002). This is opposed to a genetic technique, considering the biologic evolution as a basis for the guided Monte Carlo approach (e.g. Mallick *et al.* 1995).

The Aki and Richards formula (1980) gives access to the approximate P-wave reflectivity at the various offsets in the pre-stack domain.

$$R_{(\theta)} = 0.5 \left( \frac{\Delta V_p}{V_p} + \frac{\Delta \rho}{\rho} \right) - 2 \left( \frac{V_s}{V_p} \right)^2 \left( 2 \frac{\Delta V_s}{V_s} + \left( \frac{\Delta \rho}{\rho} \right) \sin^2 \theta + 0.5 \left( \frac{\Delta V_p}{V_p} \right) \tan^2 \theta \right) \quad (11)$$

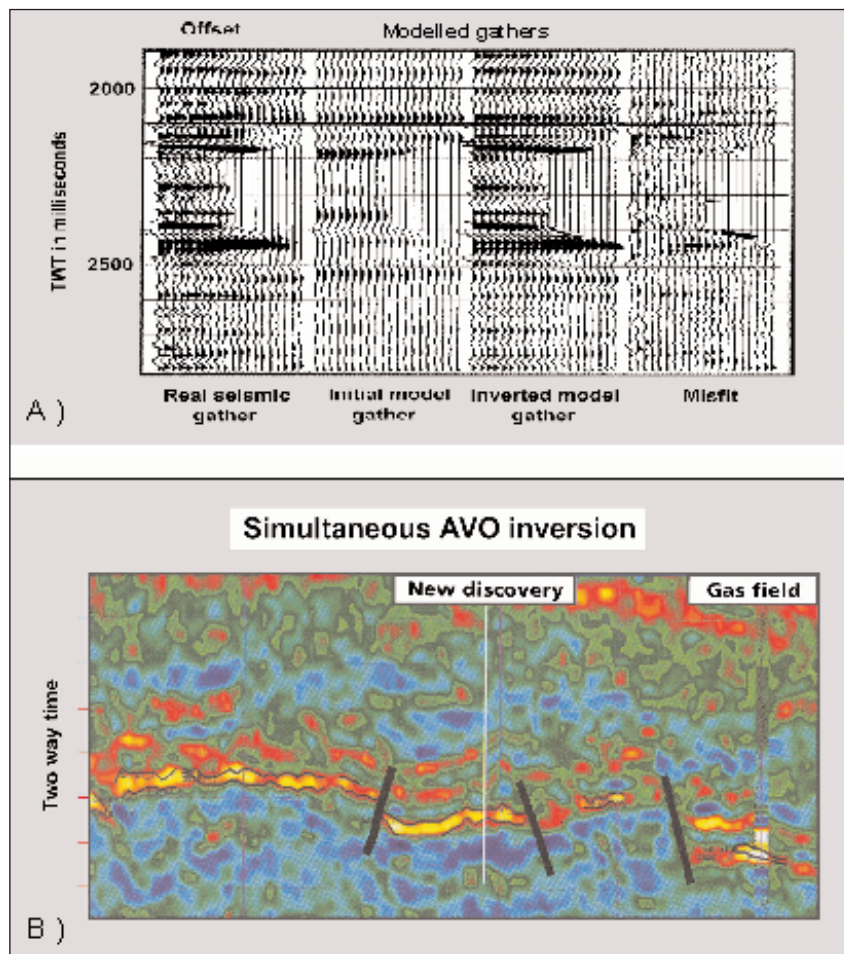


Figure 20A Simultaneous inversion is basically model-driven in approach. The Aki and Richards approximation of the Zoeppritz equations is used to compute the reflectivities at different offsets. P- and S-wave acoustic impedance models are perturbed in order to compute a new reflectivity and synthetic CDP gathers. These are compared with real seismic data and the difference is minimised by a simulated annealing technique. The advantage of the simultaneous inversion is that it avoids the limitation in the degree of the angle of incidence and the same time model is applicable for all offsets (modified after Ma 2002).

figure 20B Cross section across simultaneous inversion results. The proposed new well location was later successful in finding additional commercial hydrocarbons (courtesy Fugro-Jason Geoscience).

where  $V_p$  is the average P-velocity between two uniform half-spaces,  $V_s$  is the average S-velocity and  $\rho$  is the average density. It can be rewritten in terms of P- and S-wave impedances:

$$R_{(\theta)} = (1 + \tan^2 \theta) (\Delta I_p / 2I_p) - 8 (V_s / V_p)^2 \sin^2 \theta (\Delta I_s / 2I_s) - (\tan^2 \theta - 4(V_s / V_p)^2 \sin^2 \theta) (\Delta \rho / 2\rho) \quad (12)$$

The assumption is now made that the relative changes in  $(\Delta V_p / V_p)$ ,  $(\Delta V_s / V_s)$  and  $(\Delta \rho / \rho)$  are small and the incidence angle  $\theta$  is much less than  $90^\circ$ . This means that the second order terms can be ignored (Fatti *et al.* 1994):

$$R_{(\theta)} = (1 + \tan^2 \theta) (\Delta I_p / 2I_p) - 8 (V_s / V_p)^2 \sin^2 \theta (\Delta I_s / 2I_s) \quad (13)$$

The background  $V_s / V_p$  relationship should be known to solve this equation. If the  $V_p$  and  $V_s$  models are not good approximations of the earth model, then the linear inversion will give incorrect results. Ma (2002) proposes therefore to substitute the average  $V_s / V_p$  by the average  $I_s / I_p$  values. This  $I_s / I_p$  value is not coming from an a-priori model but is derived individually for each inversion iteration. Inversion is

done under the following assumptions:

- The earth has approximately horizontal layers.
- Each layer is described by both acoustic and shear impedances.

The reflection coefficients can be calculated for the n-th layer in the starting model in the following way:

$$\Delta I_p / 2I_p = (I_{p_n} - I_{p_{n-1}}) / (I_{p_n} + I_{p_{n-1}}) \quad (14)$$

$$\Delta I_s / 2I_s = (I_{s_n} - I_{s_{n-1}}) / (I_{s_n} + I_{s_{n-1}}) \quad (15)$$

$$(I_{s_n} + I_{s_{n-1}}) / (I_{p_n} + I_{p_{n-1}}) \quad (16)$$

These functions are utilised to compute the reflectivity at all angles in the formula above. This is convolved with the wavelet to obtain a synthetic gather. The synthetic gather is compared with the original seismic CDP gather and the misfit is computed (Figure 20A). The model is subsequently perturbed and a new comparison made to reduce the misfit. The convolution assumes a plane wave propagation across the boundaries of horizontally homogeneous layers and does not take into account geometrical divergence, non-elastic absorption, wavelet dispersion, transmission losses, mode conver-

sions and multiple reflections. These issues should have been addressed in the data pre-conditioning step.

The inversion transforms the seismic cube into reflectivity cubes for different offset ranges. Cross sections and layer maps are convenient to visualize lateral changes in the inversion results (Figure 20B). The advantage of the simultaneous inversion is that there are few constraints on the validity of the computation caused by the offset angles used. A simple initial Vp model serves as input, summarising the expected low frequency variation. This approach guarantees stability in the end-result. A density model is constructed applying Gardner's estimation (Gardner *et al* 1975) or a very simple Vp/Vs model is used (as approximation a constant value of 2). A further advantage is that the same time model is applicable for all offset angles. The calculations are usually done for six discrete offset angle ranges. The following attributes are computed: Vp, Vs, rhomu, lambdarho and Vp/Vs.

The two term Aki and Richards formula is frequently written in a simplified form (5). It gives access to the  $R_p$  and  $R_s$  reflectivities for the zero offset in the following way:

$$R_\theta = A + B \sin^2 \theta + C \sin^2 \theta \tan^2 \theta$$

$$A = 0.5 \left( \frac{\Delta V_p}{V_p} + \frac{\Delta \rho}{\rho} \right)$$

$$B = 0.5 \left( \frac{\Delta V_p}{V_p} \right) - 4 \left( \frac{V_s}{V_p} \right)^2 \left( \frac{\Delta V_s}{V_s} - 2 \left( \frac{V_s}{V_p} \right)^2 \frac{\Delta \rho}{\rho} \right)$$

$$C = 0.5 \left( \frac{\Delta V_p}{V_p} \right)$$

A is the intercept, B is the gradient in AVO analysis and C is the AVO curvature. If  $V_p / V_s = 2$ , then for the zero degree incidence angle (Russell *et al*, 2003) the two term approximation is valid and :

$$R_p 0 = A \quad (17)$$

$$R_s 0 = (A-B) / 2 \quad (18)$$

The density of the rock for the P- and S-wave is the same, but the velocity contrasts change.

Also a linearised Bayesian approach has been adopted in an AVO inversion scheme (Buland and Omre 2003). The Bayes theorem exploits the conditional probability principle. The posterior solution is given by a Gaussian probability density function, whereby the calculations are based on a Monte Carlo simulation. The linearisation is made possible by assuming weak impedance contrasts for the Zoeppritz equations. A drawback is that noise in the data has a detrimental effect on the uncertainties in the solution.

### 3. Pre-stack waveform inversion

This method is based on a wave equation forward modelling algorithm. Numerous earth models are fitted to the pre-stack response of the individual traces. The wave equation is run with converted wave energy, interbed multiples, transmission losses and P-wave reflections (Benabentos *et al*. 2002, Mallick

*et al*. 2000). It is a computing intensive method; therefore it is often combined with other non-linear estimation and correlation schemes. Neural network training is a powerful tool to convert seismic data into pseudo well log traces (e.g. Banchs and Michelena 2002). Interval confidence calculation is done in order to adopt a more statistical approach.

The first four inversion methods described above are known as **acoustic impedance inversions**. The model-driven inversion is the best suited for poor data quality surveys with limited well control (estimated sonic, estimated density, no checkshots?) as the seismic data itself is the basic guide for the inversion. Elastic inversion is labour intensive and should only be undertaken when a feasibility study has demonstrated its benefits. A shear sonic is needed or estimated, but even that is not always necessary according to Cambois (2002). His suggested fluid factor basically boils down to the behaviour of the far offset stack.

### A word of caution

As a word of warning: 'Seismic inversion is not a unique process'. There are several AI models that generate similar synthetic traces when convolved with the wavelet. The number of possible solutions is significantly reduced by putting constraints on the modelling and, in doing so, most plausible scenario is retained (Veeken *et al*. 2002, Da Silva *et al.*, in prep). The support of other investigation techniques, like AVO analysis and forward modelling, increases the confidence in the inversion results. Even a negative correlation is important information as it results in an increase of the risk attached to the prospect. It may sound a bit controversial, but ultimately it will reduce the drilling risk on the well proposals because of the better ranking criteria.

Seismic velocities are sensitive to the presence of gas in a rock sequence. A 5-10% gas saturation has already a tremendous impact on the seismic response. It will lead to AVO and AI anomalies, but these are non-commercial. The extent of the mapped anomalies should therefore always be treated with some care. AVO and inversion anomalies are likely related to the maximum distribution of hydrocarbons.

Seismic inversion depends heavily on the proper integration of well data. Incorporation of anisotropy effects in the inversion scheme will improve the quality of the output data (Rowbotham *et al*. 2003). This is especially important when dealing with deviated holes.

Seismic inversion is gradually becoming a routine processing step in field development studies as well as for exploration purposes. Even time lapse inversions are now conducted (Gluck *et al*. 2000, Oldenziel 2003). The AI attribute is gradually replacing the normal amplitude seismic representation as inversion is becoming an integral part of the reservoir characterisation workflow (cf Latimer *et al*. 2000, Van Riel 2000). The positive track record of case histories clearly demonstrates the added value of this type of seismic analysis.



## Conclusions

Inversion replaces the seismic signal by a blocky impedance response. Various seismic inversion schemes are available, each having their own advantages. Input data conditioning is an important step when quantitative interpretation is the ultimate goal. Model-driven inversion is robust, even when dealing with poor data sets. A true 3D approach stabilises the output. The probabilistic method quantifies uncertainties in the geological model and incorporates these in the end results. The shared earth model is suited as input to reservoir simulation packages. The pre-stack approach exploits AVO effects present in the seismic dataset. All of these methods have their own restrictions and limitations. Feasibility and synthetic modelling studies are recommended before starting an inversion and/or AVO project.

There is a trade-off between work involved / cost / time and quality of the end product. Seismic inversion is not a unique process, i.e. there is not a single solution to the given problem. In other words: several AI or EI models may equally well explain the same seismic response. Numerous studies have already proven the added value of inversion processing for better definition of prospects and leads, improved DHI detection, delineation of sweet spots with better porosity and permeability characteristics. All these aspects allow optimisation of field development plans with improved volumetric estimations and make for more reliable economic forecasts possible.

## Acknowledgements

We are indebted to CGG, CMG, Pemex and Jason Geoscience companies for granting permission to use their data. We thank our immediate colleagues for sharing their working ideas. In particular we want to thank Dr E. Mendez, M. Rauch-Davies, H. Bernal, G. Velasquez, A. Marhx, J. Camara, N. Van Couvering, R. Walia, J. Helgesen, M. Querne, Y. Lafet, J.M. Michel, C. Pinson, S. Addy, R. Martinez, J.L. Gelot, P. Van Riel and P. De Beukelaar (Solegeo) for their contributions. The comments of the reviewers have been highly appreciated. Special thanks is given to Dr M. Bacon for his constructive remarks.

## References

- Aki, K. and Richards, P.G. [1980] *Quantitative seismology, theory and methods*. Freeman, San Francisco, 557.
- Ajlani, G., Al Kaabi, M. and Suwainna, O. [2003] Comparative analysis ( CASP): a proposal for quantifying seismic data processing. *The Leading Edge*, **22**, 1, 46-48.
- Banchs, R. E. and Michelena, R.J. [2002] From 3D seismic attributes to pseudo-well-log volumes using neural networks: practical considerations. *The Leading Edge*, **21**, 10, 996-1001.
- Benabentos, M., Mallick, S., Sigismondi, M. and Soldo, J. [2002] Seismic reservoir description using hybrid seismic inversion: a 3D case study from the Maria Ines Oeste Field, Argentina. *The Leading Edge*, **21**, 10, 1002-1008.
- Buland, A. and Omre, H. [2003] Bayesian linearized AVO inversion. *Geophysics*, **68**, 1, 185-198.
- Cambois, G. [2000] AVO inversion and elastic impedance. *Expanded abstracts, 70th SEG Annual Meeting*, Calgary, 1-4.
- Castagna, J.P. and Backus, M.M. [1993] Offset dependent reflectivity – Theory and practice of AVO analysis. SEG, Tulsa, Investigations in Geophysics 8, 348.
- Connolly, P. [1999] Elastic impedance, *The Leading Edge*, **18**, 4, 438-452.
- Cook, D.A. and Snieder, W.A. [1983] Generalized linear inversion of reflection seismic data. *Geophysics*, **48**, 665-676.
- Cosentino, L. [2001] *Integrated reservoir studies*. Technip, Paris, 310.
- Coulon, J.P., Duboz, P. and Lafet, Y. [2000] Moving from seismic to layered impedance cube and porosity prediction in the Natih E member. *GeoArabia*, **5**, 1, 72-73.
- Da Silva, M., Rauch-Davies, M., Soto Cuervo, A. and Veeken, P. in prep. , Pre- and post-stack attributes for enhancing production from Cocuite gas reservoirs. *66th EAGE Annual Conference*, Paris [2004]
- Da Silva, M., Rauch-Davies, M., Soto Cuervo, A. and Veeken, P. in prep. , Data conditioning for a combined inversion and AVO study. *66th EAGE Annual Conference*, Paris, [2004]
- Dix, C.H. [1955] Seismic velocities from surface measurements. *Geophysics*, **20**, 68-86.
- Duboz, P., Lafet, Y. and Mougenot, D. [1998] Moving to layered impedance cube: advantages of 3D stratigraphic inversion. *First Break*, **17**, 9, 311-318.
- Dubrule, O. [2003] Geostatistics for seismic data integration in earth models. *EAGE distinguished instructor series* **6**, 282.
- Dutta, N.C. [2002] Geopressure prediction using seismic data: Current status and the road ahead. *Geophysics*, **67**, 6, 2012-2041.
- Fabre, N., Gluck, S., Guillaume, P. and Lafet, Y. [1989] Robust multichannel strati-graphic inversion of stacked seismic traces, *59th Annual Meeting SEG*, 943.
- Fatti, J.L., Smith, G.C., Vail, P.J., Strauss, P.J. and Levitt, P.R. [1994] Detection of gas in sandstone reservoirs using AVO analysis.: A 3-D seismic case history using the Geostack technique. *Geophysics*, **59**, 1362-1376.
- Faust, L.Y. [1951] Seismic velocity as a function of depth and geologic time. *Geophysics*, **16**, 192-206.
- Faust, L. Y. [1953] A velocity function including lithologic variations. *Geophysics*, **18**, 271-287.
- Gardner, G.H.F., Gardner, L.W. and Gregory, A.R. [1974] Formation velocity and density - The diagnostic basics for stratigraphic traps, *Geophysics*, **39**, 770-780.
- Gluck, S., Juve, E. and Lafet, Y. [1997] High resolution impedance layering through 3D stratigraphic inversion of post stack seismic data. *The Leading Edge*, **16**, 1309- 1315.
- Gluck, S., Deschizeaux, B., Mignot, A. Pinson and Huguet, F. [2000] Time-lapse impedance inversion of post-stack seismic data. *Expanded abstracts, 70th Annual Meeting SEG*, Calgary, 1509-1512.
- Goffe, W.L., Ferrier, G.D. and Rodgers, J. [1994] Global optimisation of statistical functions with simulated annealing. *Journal of*

*Econometrics*, 60, 65-100.

- Goodway, W., Chen, T. and Downton, J. [1997] Improved AVO fluid detection and lithology determination using Lamé's petrophysical parameters: LambdaRho, MuRho and Lambda/Mu fluid stack from P and S inversions. *Canadian Society of Exploration Geophysicists, Abstracts*, 148-151.
- Haas, A. and Dubrule, O. [1994] Geostatistical inversion – a sequential method of stochastic reservoir modelling constrained by seismic data. *First Break*, 12, 11, 561-569.
- Hardage, B.A., [1985] Vertical seismic profiling - a measurement that transfers geology to geophysics: in Berg O.R. and Woolverton D.G. (eds) [1985], *Seismic stratigraphy II: an integrated approach to hydrocarbon exploration*, AAPG Memoir 39, AAPG, Tulsa, 13-34.
- Helland-Hansen, D., Magnus, I., Edvardsen, A., and Hansen, E. [1997] Seismic inversion for reservoir characterisation and new well planning in the Snorre field. *The Leading Edge*, 16, 3, 269-273.
- Lancaster, S. and Whitcombe, D. [2000] Fast track "coloured" inversion. *Expanded abstracts, 70th SEG Annual Meeting*, Calgary, 1572-1575.
- Latimer, R.B., Davison, R. and Van Riel, P. [2000] Interpreter's guide to understanding and working with seismic derived acoustic impedance data. *The Leading Edge*, 19, 3, 242-256.
- Lindseth, R. [1979] Synthetic sonic logs - a process for stratigraphic interpretation. *Geophysics*, 44, 3-26.
- Ma, X. [2002] Simultaneous inversion of prestack seismic data for rock properties using simulated annealing. *Geophysics*, 67, 1877-1885.
- Mallick, S. [1995] Model-based inversion of amplitude variations with offset data using a genetic algorithm. *Geophysics*, 60, 939-954.
- Mallick, S., Lauve, J. and Ahmad, R. [2000] Hybrid seismic inversion: A reconnaissance tool for deep water exploration. *The Leading Edge*, 19, 38-43.
- Mari, J.L., Glangeaud, F. and Coppens, F. [1999] *Signal processing for geologists and geophysicists*. Editions Technip, Paris, 480
- Metropolis, N., Rosenbluth, A., Rosenbluth, M., Teller, M., and Teller, E. [1953] Equation of state calculations by fast computing machines. *Journal Chem Phys*, 21, 1087-1092.
- Oldenziel, T. [2003] Time lapse seismic within reservoir engineering. *Thesis, Delft University of Technology*, 204.
- Onderwater, J., Wams, J. and Potters, H. [1996] Geophysics in Oman. *GeoArabia*, 1, 2, 299-324.
- Pendrel, J., Stewart, R.R. and Van Riel, P. [1998] Interpreting sand channels from 3C-3D seismic inversion. *Expanded Abstracts, 71th SEG Annual Meeting*, 1588-1591.
- Pica, A., Diet, J. and Tarantola, A. [1990] Non linear inversion of seismic reflection data in a laterally invariant medium. *Geophysics*, 55, 284-292.
- Ronghe, S. and Surarat, K. [2002] Acoustic impedance interpretation for sand distribution adjacent to a rift boundary fault, Suphan basin, Thailand. *AAPG Bulletin*, 86, 10, 1753-1771.
- Rowbotham, P., Marion, D., Eden, R., Williamson, P., Lamy, P. and Swaby, P. [2003] The implications of anisotropy for seismic impedance inversion. *First Break*, 21, 53-57.
- Russell, B.H., Hedlin, K., Hilterman, F.J. and Lines, L.R. [2003] Fluid property discrimination with AVO: A Biot-Gassmann perspective. *Geophysics*, 68, 1, 29-39.
- Sheriff, R.E. [2002] *Encyclopedic dictionary of exploration geophysics*. SEG, Tulsa, 429.
- Shuey, R.T. [1985] A simplification of the Zoeppritz equations. *Geophysics*, 50, 609-614.
- Stewart, R.R., Gaiser, J.E., Brown, R. and Lawton, D.C. [2003] Converted-wave seismic exploration: applications. *Geophysics*, 68, 1, 40-57.
- Sylta, O. and Krokstad, W. [2003] Estimation of oil and gas column heights in prospects using probabilistic basin modelling methods. *Petroleum Geoscience*, 9, No. 3, 243-254.
- Tarantola, A. [1984] Inversion of seismic reflection data in the acoustic approximation. *Geophysics*, 49, 1259-1266.
- Tarantola, A. [1986] A strategy for non linear elastic inversion of seismic reflections data. *Geophysics*, 51, 1893-1903.
- Torres-Verdin, C., Victoria, M., Merletti, G. and Pendrel, J. [1999] Trace-based and geostatistical inversion of 3-D seismic data for thin sand delineation: An application in San Jorge Basin, Argentina. *The Leading Edge*, 18, 9, 1070-1077.
- Trad, D., Ulrych, T. and Sacchi, M. [2003] Latest views of the sparse Radon Transform. *Geophysics*, 68, 1, 386-399.
- Van der Laan, J. and Pendrel, J. [2001] Geostatistical simulation of porosity and risk in a Swan Hills reef. *Expanded abstracts, 71th SEG Annual Meeting*, 1588-1591.
- Van Riel, P. [2000] The past, present and future of reservoir characterization. *The Leading Edge*, 19, 8, 878-881.
- Vazquez, R., Mendoza, A., Lopez, A., Linares, M. and Bernal, H. [1997] 3-D seismic role in the integral study of the Arcabuz-Culebra field, Mexico. *The Leading Edge*, 16, 12, 1763-1766.
- Veeken, P.C.H., (in prep.), *Seismic stratigraphy, basin analysis and reservoir characterisation*. Elsevier, Amsterdam, 350.
- Veeken, P.C.H., Rauch, M., Gallardo, R., Guzman, E. and Vila, R. Villaseñor [2002] Seismic inversion of the Fortuna National 3D survey, Tabasco, Mexico. *First Break*, 20, 5, 287-294.
- Velzeboer, C.J. [1981] The theoretical seismic reflection response of sedimentary sequences. *Geophysics*, 46, 843-853.
- Walden, A.T. and Hosken, J.W.J. [1985] An investigation of the spectral properties of primary reflection coefficients. *Geophysical Prospecting*, 33, 400-435.
- Weber, K.J. and Van Geuns, L.C. [1990] Framework for constructing clastic reservoir simulation models. *Journal of Petroleum Technology*, 42, 10, 1248-1297.
- White, R. and Simm, R. [2003] Tutorial: Good practice in well ties. *First Break*, 21, 10, 75-83.
- Yilmaz, O. [1987] Seismic data processing, Society of Exploration Geophysicists, *Investigations in geophysics*, 2, Tulsa, SEG, 526.
- Yilmaz, O. [2001] *Seismic data analysis, Volume 1 and 2*. Society of Exploration Geophysicists, *Investigations in geophysics*, 10, Tulsa, SEG, 2027.
- Zoeppritz, K. [1919] *On the reflection and propagation of seismic waves*, *Erdbebenwellen VIII*, Gottinger Nachrichten I, 66-84.